UNIVERSITY OF KWAZULU-NATAL

RELATIVISTIC ASTROPHYSICAL MODELS OF PERFECT AND RADIATING FLUIDS

NARENEE MEWALAL

Relativistic Astrophysical Models of Perfect and Radiating Fluids

by

Narenee Mewalal

Submitted in fulfilment of the

academic requirements for the degree of

Doctor of Philosophy

in the

School of Mathematics, Statistics and Computer Science

University of KwaZulu-Natal

Durban

January 2019

As the candidate's supervisors we have approved this dissertation for submission.

Prof S Hansraj Signed: Date: 27/03/2019

Prof M Govender Signed: Date: 27/03/2019

Abstract

In this thesis we seek solutions of the classical Einstein field equations describing astrophysical bodies composed of perfect and imperfect fluids. We firstly investigate a simple Petrov type D spacetime with a perfect fluid source. The equations of motion are generated and exact solutions are obtained utilising the conformal transformation technique. While the seed metric is known to suffer physical pathologies, the transformed system offers rich classes of solutions. These solutions are examined for physical reasonableness with the aid of graphical plots for the static and nonstatic cases. Specialising to a spacetime foliation in the temporal coordinate and one spatial coordinate leads to solutions of the hyperbolic trigonometric type. Additionally, we analyse perfect fluid models under the assumption that the spacetime is described by a plane symmetric line element which is conformal to the isotropic Kasner solution. The matter source for these models is described by a perfect fluid with nonvanishing pressure. An exact solution is located describing the gravitational field within a plane symmetric fluid. Three-dimensional graphical plots show that the model displays the necessary qualitative features for physical reality. The third class of models represents radiating fluid spheres within the framework of general relativity. By employing a perturbative scheme together with a linear equation of state, we generate a dynamical model of radiative collapse. The stability of these models are investigated by varying the equation of state parameter.

I dedicate this work to

my beautiful little

Leia

Despite all that I have read about in the literature, you remain the brightest star known to me. This is a small accomplishment in comparison with what you are going to achieve - of that, I am certain

FACULTY OF SCIENCE AND AGRICULTURE

DECLARATION 1 - PLAGIARISM

I, Narenee Mewalal, student number: 201509798, declare that

1. The research reported in this dissertation, except where otherwise indicated, is my original research.
2. This work has not been submitted for any degree or examination at any other university.
3. The investigative work in this dissertation does not contain other persons data, pictures, graphs or other information, unless specifically acknowledged as being sourced from other persons.
4. This study does not contain other persons' writing, unless specifically acknowledged as being sourced from other researchers. Where other written sources have been quoted, then:
   a. their words have been re-written but the general information attributed to them has been referenced
   b. where their exact words have been used, their writing has been placed in italics or within quotation marks, and referenced.
5. This dissertation does not contain text, graphics or tables copied and pasted from the Internet, unless specifically acknowledged, with the source being detailed in the Bibliography.

Signed: Date: 27/03/2019

FACULTY OF SCIENCE AND AGRICULTURE

DECLARATION 2 - PUBLICATIONS

Publication 1

Hansraj S, Govinder K S and Mewalal N, Conformal mappings in relativistic astrophysics, *J. Appl. Math* **2013**, 196385 (2013).

Publication 2

Hansraj S, Govender M and Mewalal N, Expanding, shearing and accelerating isotropic plane symmetric universe with Kasner geometry, *Mod. Phys. Lett. A.* **33**, 1850143 (2018).

Publication 3

Govender M, Mewalal N and Hansraj S, The role of an equation of state in the dynamical (in)stability of a radiating star, *Eur. Phys. J. C.* **79**, 24 (2019).

Acknowledgements

I wish to express my appreciation to the following people and organisations who made this dissertation possible:

- My husband Arvin: we tend to take for granted the people who we love the most, yet you unconditionally remain a source of strength to me. This work is a symbol not only of my sacrifices, but of yours too. I thank you from the bottom of my heart.

- Prof S Hansraj for your expert guidance, support and patience in waiting for me to complete this project.

- Prof M Govender: it is said that kind words builds confidence in people. I thank you for sharing your knowledge and for accompanying me on this journey with kindness, compassion and humility. You are a true professional.

- Prof KS Govinder for your valuable contribution to the work on conformal mappings and Lie symmetries.

- My children Nikoshia, Nikhil, Hollis and Leia: your patience whilst having to contend with an all too busy mum for much of the past year is very much appreciated. I am all yours now.

- I thank the TDG-NCP for funding in respect of sabbatical leave without which the completion of this work would not have been possible.

- Prof DB Lortan, head of department of Mathematics at the Durban University of Technology, for your continued support, interest and words of encouragement.

- Prof S Moyo and the research team at Durban University of Technology for your ongoing support.

- In my final and most important word of thanks, I express my heartfelt gratitude to my mother and late dad: you may not have had direct involvement in this work, but your contribution to my studies cannot be understated. You so selflessly provided me with the means to an education despite your financial limitations. Without that foundation I could never have come this far. Thank you.

Contents

Chapter 1

Introduction

Since the dawn of time, the tiny world that we were born into has been a mystery to mankind. Who are we? Where did we come from and how did our universe come into being? What is the age and the size of the cosmos? For many, and for a long time, the idea of a universe was earth itself - our home. It turns out that the answers to these questions were always there, but we did not see them until we devised more powerful means of seeing. The story of this awakening has many beginnings, with many heroes and from various times and places. Each of these men and women brought us a little closer to unlocking the secrets of the universe. But one man, and a single mathematical sentence, changed our understanding of the universe on the largest of scales.

Referred to by some as "the icon of genius", Albert Einstein brought to us one of the greatest feats in modern physics, his theory of general relativity. For some two hundred years earlier Newton's laws of motion, in which gravity was taken to be a force of attraction between two bodies, was the most successful theory of gravitation. Then, early in the twentieth century Einstein's revolutionary ideas on space, time and gravitation made an appearance. According to Einstein, space and time are interwoven into a single continuum which he referred to as spacetime. Soon after publishing his theory of special relativity in 1905, Einstein began the search for a relativistic theory that would incorporate his notions of gravity and gravitation. Starting with a simple thought experiment in 1907 about an observer in free fall, he embarked on a journey that would last eight years, culminating in his 1915 presentation of what we now know as the Einstein field equations.

Around that period the physics community was caught up in quantum mechanics and particle physics which were new frontiers at the time. By comparison, general relativity did not appear to be much more than minor amendments of the Newtonian gravitation theory. Its mathematics appeared to be too difficult for most to understand, and it offered little promise for experimental evidence. It was only from the late 1950's and more especially in the 1960's that the topic started to be rejuvenated. As phenomena such as quasars, pulsars and microwave background radiation, which were predicted by general relativity, started to be discovered, the theory gained recognition. Researchers began to realise its implications for explaining various physical phenomena. However, at the heart of these explanations and predictions was the mathematics in the form of the Einstein field equations. In this regard, new mathematical techniques which streamlined the calculations in general relativity started to surface, making it easier to visualise its concepts.

In recent times, the quest for exact solutions of Einstein's equations has shifted from a purely mathematical exercise into the arena of modeling of objects based on the observational and experimental data available. Many well known stellar models are the result of exact solutions of the field equations. Schwarzschild's (1916a) vacuum exterior solution describes the gravitational field outside a bounded spherical mass and is a useful approximation for describing astrophysical objects such as non-radiating stars. In contrast, the Vaidya (1951) metric describes the non-empty exterior spacetime of a spherically symmetric radiating star. The static solution of the Einstein-Maxwell field equations by Reissner (1916) and Nørdstrom (1918) corresponds to the gravitational field of a charged non-rotating spherically symmetric object. The Kerr metric (1963) is an exact solution of the Einstein field equations which describes the geometry of a vacuum spacetime exterior to a rotating, uncharged sphere. The charged version of the rotating sphere was obtained by Kerr (1963) and Newman (1965).

Stars are the most suitable candidates for studying the theory of general relativity, since this theory was first validated by the famous experiment in which the deflection of light from the stars by the sun was measured during a solar eclipse. In particular, the ultimate fate of a radiating star undergoing gravitational collapse is a topic of much research. A star could end its journey as a white dwarf if its mass is below that of the Chandrasekhar (1964) limit of approximately 1.3 solar masses. A star could also take the form of a neutron star if its mass does not exceed the Tolman-Oppenheimer-Volkoff (TOV) limit (1939) which is roughly $3M_\odot$, where $M_\odot$ refers to the mass of the sun. In the event that the star does not achieve stability as a white dwarf or as a neutron star, it will continue to collapse under the influence of gravity, resulting in the formation of a black hole. Pioneering work on black holes was done by, amongst others, Roger Penrose (1965) and Stephen Hawking (1970). Specifically, it was shown by Hawking and Penrose that a star's evolution is completely determined by its mass, charge and angular momentum and this is known as the "No-hair" theorem. Since the first study on gravitational collapse was carried out by Oppenheimer and Snyder (1939), many improvements have been made in an attempt to obtain physically realistic astrophysical models. For example, the inclusion of shear was investigated by Govender *et al* (2014). However, these additions such as shear, anisotropic stresses, charge, and so on, often complicate the process of solving the field equations. Hence various methods, some of which include physically justifiable assumptions such as vanishing shear and the imposition of an equation of state, have been adopted.

Investigating the stability of a collapsing star is an important component of general relativity research. In this regard, the Chandrasekhar (1964) adiabatic stability index proves to be a useful tool. In addition, the sound-speed index also serves as a stability measure. Violation of causality corresponds to an unstable stellar distribution.

Despite the many developments in general relativity over the past century, a number of open problems remain. For example, our understanding of pulsars is incomplete since there exists no known interior solution that matches the rotating vacuum Kerr metric. The mathematical problem in this instance pertains to the lack of understanding of the concept of frame-dragging, also known as the Lense-Thirring effect which was discussed in a paper by Pfister (2007). Also, in as far as exact solutions with respect to spatial symmetry is concerned, spherically symmetric spacetimes have been thoroughly researched, with the examples listed in the previous paragraph being just a few of the many works conducted on spherical symmetry. However, there is a paucity of investigations into non-spherically symmetric spacetimes such as cylindrically symmetric and plane symmetric spacetimes. Plane symmetric objects and universes have been studied by Taub (1951) for the static case and Kasner (1921) in the time-dependent case. The recent discovery of gravitational waves by the Laser Interferometer Gravitational Observatory (LIGO), investigated by Abbott *et al* (2016) has resulted in an increased interest in plane symmetric spacetimes. It is well known by the theorem of Jebsen (1921) and Birkhoff (1923) that spherically pulsating objects do not emit gravitational waves. Consequently, investigations of fluids with less symmetry are of importance. Note that an exact solution modeling a gravitational wave is still unknown.

The search for exact solutions of Einstein's equations remains an ongoing process, for concealed inside the innocuous looking equation are actually ten partial differential equations which are nonlinear, coupled and, in general, difficult to solve. So in order to achieve success in solving these equations, it becomes necessary to introduce prescriptions to simplify the problem to a tractable level. Various *ad hoc* assumptions mentioned in Stephani *et al* (2003) are made on the spacetime geometry or on the matter content. All of the best known solutions have been obtained by making some assumption, mostly on the spacetime symmetry as listed in the above paragraph.

An alternate, more systematic approach is to utilise the method of conformal mappings whereby new and unique solutions are generated from existing ones, known as seed metrics. In one of the first papers that demonstrated the use of conformal transformations, Buchdahl (1971) proved the conformal flatness of the Schwarzschild interior solution by performing a conformal transformation on Minkowski space into the Schwarzschild interior solution. A simple consequence of this method is that, by a conformal transformation of the Minkowski space the Schwarzschild interior solution may be generated. We note that, in this example, a perfect fluid solution is generated from a seed metric which is not a perfect fluid. The advantage of the conformal mappings method is that physically reasonable new solutions may be generated from seed metrics which are possibly defective. The point is that these metrics already solve the Einstein field equations, and what remains is to solve the modified part due to the conformal transformation. This is one of the routes pursued in this work.

This dissertation is organised as follows:

- Chapter 2: This chapter focuses on some of the key concepts pertaining to general relativity which are necessary for the remainder of this dissertation.

- Chapter 3: This chapter represents the work done for the first publication by Hansraj *et al* (2013) towards the doctoral qualification. The main focus of this chapter is the method of conformal mappings as a solution-generating tool. We use Lie group analysis to generate the Einstein field equations for a perfect fluid matter configuration. Exact static and nonstatic solutions are found. These solutions are examined for acceptability as realistic distributions of matter. In particular, we investigate the positive definiteness of the energy density and pressure, the causality criterion, existence of a vanishing pressure hypersurface and stability of the solution.

- Chapter 4: We examine plane symmetric spacetimes and, via a conformal mapping, construct a nonstatic perfect fluid model using the plane symmetric anisotropic Kasner metric as a seed solution. The solution is shown to be accelerating, expanding and shearing. The publication by Hansraj *et al* (2018) is contained in this chapter.

- Chapter 5: With reference to a spherically symmetric shear-free isotropic spacetime we investigate the effect of an equation of state on the stability of a radiating star undergoing dissipative collapse. A perturbative scheme is employed to study the collapse of an initially static star described by the interior Schwarzschild solution. We impose a linear equation of state of the form $p_r = \gamma\mu$. The link between the equation of state parameter γ and the stability index Γ is investigated for the Newtonian and post-Newtonian regimes. The publication by Govender *et al* (2019) forms the basis of this chapter.

- Chapter 6: Conclusion and discussion of results.

Chapter 2

General Relativity

In this chapter we provide a brief overview of the mathematics required for general relativity. In §2.1 the preliminary concepts in differential geometry are outlined. The energy-momentum tensor for fluids in various forms is given in §2.2, and in §2.3 we present the Einstein field equations.

2.1 Differential Geometry

The mathematical formalism underpinning the notion of curved spacetimes as described by the theory of general relativity is known as differential geometry. Space and time are represented as a four-dimensional manifold which is continuous and differentiable at all points, together with a symmetric, nonsingular metric field **g** with signature $(-+++)$. An event or point on this spacetime manifold is represented by the vector $(x^a) = (x^0, x^1, x^2, x^3)$ where x^0 is the temporal coordinate and x^1, x^2, x^3 are the spatial coordinates.The invariant distance between two neighbouring events of a curve in the manifold is defined by the fundamental metric form

$$ds^2 = g_{ab}dx^a dx^b.$$

which is commonly referred to as the line element. The Christoffel symbol Γ is a metric connection coefficient that preserves inner products under parallel transport of a vector field, and is expressed in terms of the metric tensor and its derivatives in the following way :

$$\Gamma^a{}_{bc} = \tfrac{1}{2} g^{ad}(g_{cd,b} + g_{db,c} - g_{bc,d}), \tag{2.1.1}$$

where commas denote partial differentiation. The Riemann curvature tensor is the central object in the study of curved surfaces and encodes all the information characterising the geometry of the tensor fields. It is a $(1,3)$ tensor field constructed from the connection coefficients (2.1.1) and is given by

$$R^a{}_{bcd} = \Gamma^a{}_{bd,c} - \Gamma^a{}_{bc,d} + \Gamma^a{}_{ec}\Gamma^e{}_{bd} - \Gamma^a{}_{ed}\Gamma^e{}_{bc}, \tag{2.1.2}$$

The vanishing of $R^a{}_{bcd}$ denotes a flat surface. Contraction of the Riemann tensor (2.1.2), with the use of the metric tensor g_{ab}, generates the Ricci tensor R_{ab} which is expressed as

$$R_{ab} = \Gamma^d{}_{ab,d} - \Gamma^d{}_{ad,b} + \Gamma^e{}_{ab}\Gamma^d{}_{ed} - \Gamma^e{}_{ad}\Gamma^d{}_{eb}. \tag{2.1.3}$$

A further contraction of the Ricci tensor (2.1.3) yields the Ricci scalar

$$R = g^{ab} R_{ab} = R^a{}_a. \tag{2.1.4}$$

The Ricci tensor and the Ricci scalar contain information about "traces" of the Riemann tensor. It is sometimes useful to consider separately those aspects of the Riemann tensor which are not informed by the Ricci tensor. In this regard, we mention the Weyl conformal tensor which is the traceless component of the Riemann tensor. It is given in n dimensions by

$$\begin{aligned} C_{abcd} \quad &= \quad R_{abcd} + \tfrac{1}{(n-1)(n-2)} R(g_{ac}g_{bd} - g_{ad}g_{bc}) \\ &\quad - \tfrac{1}{n-2}(g_{ac}R_{bd} - g_{bc}R_{ad} + g_{bd}R_{ac} - g_{ad}R_{bc}) \ . \end{aligned}$$

The vanishing of the Weyl tensor denotes a conformally flat surface, meaning that the metric is a scalar function multiple of Minkowski space.

2.2 Energy–momentum Tensor

The energy–momentum tensor determines the amount of mass-energy which is contained in a unit volume. The curvature of spacetime, which is quantified by the Einstein tensor G_{ab}, is a result of mass-energy.

A perfect fluid is a continuum of matter with no heat conduction and no viscosity. It is completely characterized by its pressure and density. For a perfect fluid, the energy–momentum tensor T_{ab} is given by

$$T_{ab} = (\mu + p)u_a u_b + p g_{ab} \tag{2.2.1}$$

For matter in its neutral state, the energy–momentum tensor is given by

$$T_{ab} = (\mu + p)u_a u_b + p g_{ab} + q_a u_b + q_b u_a + \pi_{ab} \tag{2.2.2}$$

where μ is the energy density, p is the isotropic pressure, q_a is the heat flow vector, u_a the velocity field vector and π_{ab} is the stress tensor.

If any of the following are present within the fluid: bulk viscosity, shear stress, heat flow, anisotropic pressure and free-streaming radiation, we refer to the matter distribution as an imperfect fluid. The energy-momentum tensor for an imperfect fluid, as given by Herrera *et al* (2009), is

$$T_{ab} = (\mu + p_t + \Pi)\, V_a V_b + (p_t + \Pi)\, g_{ab} + (p_r - p_t)\, \chi_a \chi_b + q_a V_b + q_b V_a + \epsilon l_a l_b + \pi_{ab} \tag{2.2.3}$$

where μ is the energy density, p_r and p_t are respectively the radial and tangential pressures, π is the bulk viscosity, V^a is the comoving timelike fluid four-velocity, χ_a is a radial four-vector, q_a is the heat flux, ϵ is the null radiation density, l_a is the null four-vector and π_{ab} is the shear viscosity tensor. These quantities have the following properties :

$$V^a V_a = -1, \qquad V^a q_a = 0, \qquad l^a V_a = -1, \qquad l^a l_a = 0, \tag{2.2.4a}$$

$$\chi^a \chi_a = 1, \qquad \chi^a V_a = 0, \qquad \pi_{ab} V^b = 0, \qquad \pi_{[ab]} = 0, \tag{2.2.4b}$$

$$\pi^a_a = 0, \tag{2.2.4c}$$

where $[ab]$ implies antisymmetrisation with respect to indices a, b.

In a vacuum, which indicates an absence of matter,

$$T_{ab} = 0 \tag{2.2.5}$$

The simplest matter field worthy of interest is referred to as dust, consisting of noninteracting particles with zero pressure ($p = 0$).

2.3 Einstein Field Equations

The Einstein tensor G_{ab} is a rank two symmetric tensor which measures the rate of change of volume of particles falling freely from rest in spacetime. The Einstein tensor is obtained from the Ricci tensor (2.1.3) and the Ricci scalar (2.1.4) as follows :

$$G_{ab} = R_{ab} - \tfrac{1}{2}Rg_{ab} + \Lambda g_{ab}, \tag{2.3.1}$$

where Λ is the cosmological constant.

The history of the cosmological constant Λ is almost as long as that of general relativity. When Einstein first presented the gravitational field equations in 1915, there was no cosmological term. Two years later, in an attempt to conform to the idea of a static universe which was a largely accepted belief at the time, Einstein modified his initial equation by introducing the Λ-term. In the years that followed, the evidence provided by Lemaître, Hubble and others of a dynamic expanding universe, lead Einstein to abandon the cosmological constant, declaring it the "biggest blunder of his life". However, the removal of the cosmological term did not signify its demise. Recently the Λ-term made a reappearance in an attempt to explain observations that point to a mysterious form of energy coined "dark energy". According to Peebles and Ratra (2003), it is hypothesized that the presence of dark energy has the effect of accelerating the expansion of the universe. From an astrophysical perspective, we take $\Lambda = 0$ and so

$$G_{ab} = R_{ab} - \tfrac{1}{2}Rg_{ab} \tag{2.3.2}$$

A significant characteristic of the Einstein tensor is that its covariant derivative vanishes, and hence has the form

$$G^{ab}{}_{;b} = 0, \tag{2.3.3}$$

where semicolons denote covariant differentiation. It is worth noting that (2.3.3) is known as the contracted Bianchi identity which illustrates that the Einstein tensor is divergence-free, and so satisfies the requisite for the local conservation of energy and momentum.

Einstein established the link between the Einstein tensor, which describes the geometry of spacetime, and the energy–momentum tensor, which is a description of the matter content. Misner *et al* (1973) mention in their book entitled Gravitation that, according to Einstein, "*Space acts on matter, telling it how to move. In turn, matter reacts on space, telling it how to curve*". This relationship resulted in the formulation of one of the most powerful equations in physics, the Einstein field equations, which are expressed as

$$G_{ab} = \kappa T_{ab}, \tag{2.3.4}$$

Throughout this dissertation we utilise standard geometrical units in which the coupling constant $\kappa = 8\pi G/c^4$, the velocity of light c and the gravitational constant G are taken to be unity. (2.3.4) represents a system of ten partial differential equations which, due to coupling and nonlinearity, are difficult to integrate. However, a solution of this system of equations is necessary for the study of general relativity. We have provided only a brief exposé of the necessary mathematical framework. A comprehensive treatment of differential geometry and manifold structure applicable to general relativity may be found in de Felice and Clark (1990), Hawking and Ellis (1973) and Joshi (1993).

Chapter 3

Conformally Related Spherical Spacetimes

3.1 Introduction

Exact solutions of the Einstein field equations provide a means to the understanding of the universe, its evolution and the various relativistic phenomena that have become subjects of interest and investigation since the theory of general relativity was developed. These are a system of ten highly coupled partial differential equations expressing an equivalence between matter and geometry. Whilst the field equations hold the key to unlocking so many of the mysteries of our universe, the process is by no means easy. As the equations are difficult to solve, simpler cases have to be considered in order to gain an understanding into how certain types of matter behave under the influence of the gravitational field. In this regard, one of the most studied matter configurations mentioned in Delgaty and Lake (1998) is that of a static spherically symmetric perfect fluid. Perfect fluid is a first step towards realistic stellar model building. The assumption of spherical symmetry results in the reduction of the field equations to a system of three equations in four unknowns if the matter is neutral. However, even for this simple type of matter distribution, very few solutions are known, and even fewer of these known solutions satisfy the requirements for physical relevance.

The pioneering work of Karl Schwarzschild (1916a) resulted in the first exact solution. Even though significant advances have been made in the field of general relativity since its inception, Schwarzschild's exterior vacuum solution continues to be used to model phenomena such as gravitational collapse, black holes and singularities. This solution is unique, and moreover Birkhoff (1923) showed that the solution is independent of whether the sphere is static or not. In other words, the Schwarzschild exterior solution is simply a consequence of the spherical geometry. From this theorem also follows the conclusion that pulsating fluid spheres do not generate gravitational waves. This motivates the study of non-spherical geometry which we pursue in a subsequent chapter. By considering the case of a uniform density sphere, Schwarzschild (1916b) found a unique interior solution representing incompressible matter. However, the problem of finding all possible solutions for a non-constant energy density is still an area of active research since the field equations are underdetermined. Hence one of the geometric or dynamical variables must be specified at the start. With this freedom of choice, finding all possible solutions becomes an impractical task.

Wyman (1949) obtained general solutions of the Einstein field equations for radially symmetric matter distributions, and showed that the previously known solutions were just special cases of the general solutions he had generated. More recently, algorithmic techniques for finding all possible solutions have been introduced by several authors. Some of these include Fodor (2000), Rahman and Visser (2002), Lake (2003), Martin and Visser (2004) and Boonserm *et al* (2005), to name a few. In any case, even if solutions to the field equations are obtained, they must satisfy certain physical requirements in order to be considered candidates for realistic matter. Delgaty and Lake (1998) conducted a detailed examination of the exact solutions presented in the literature and tested them for physical plausibility. The conditions that these solutions were subjected to were: pressure isotropy, regularity at the origin, positivity of pressure and energy density at the origin, vanishing pressure at a finite boundary, monotonic decrease of the pressure and energy density to the boundary and subluminal adiabatic sound-speed. They listed 127 solutions and, at the time of the study, 16 solutions satisfied the first five criteria with only 9 having satisfied the additional sixth condition of subluminal sound-speed.

Several mathematical approaches have been used in an attempt to obtain pleasing solutions to the system of field equations. These include choosing, at the outset, functional forms for some of the variables which allows for integration of the entire system. Then there is the technique of imposing an equation of state which describes a relationship between the pressure and energy density. However, when considering non-static (time-dependent) solutions, the mathematical complexity increases. The partial differential equations are now expressed in terms of both spatial and temporal coordinates. To determine exact solutions of such systems usually amounts to prescribing relationships between the geometric quantities. In order to tackle the increased level of complexity, we utilise the alternative approach of conformal mappings. We employ conformal mappings on existing solutions possessing Killing algebras with the intention of solving the now conformally related Einstein field equations. The reason for the potential success of this approach is that the existence of conformal Killing vectors are known to simplify the field equations significantly. Conformal transformations on metric spaces adopt a mathematical approach in which new solutions may be obtained from existing ones. Note that Coley and Tupper (1994) devised a useful classification scheme for metrics based on their conformal Killing structure.

The method of Lie group analysis of ordinary differential equations is often used to obtain new group invariant solutions. In our approach, the procedure is aided by the Defrise-Carter (1975) theorem which specifies how conformal Killing vectors become Killing vectors under conformal transformations. The theorem, mentioned in Hall and Steele (1991), states: Suppose that a manifold $(M, \mathbf{g})$ is neither conformally flat nor conformally related to a generalised plane wave. Then a Lie algebra of conformal Killing vectors on M with respect to $\mathbf{g}$ can be regarded as a Lie algebra of Killing vectors with regard to some metric on M conformally related to $\mathbf{g}$. Lie groups, named after Sophus Lie who laid the foundation for the theory of continuous transformation groups, are indispensable tools for many aspects of mathematics and physics. Since a Lie group is a smooth manifold, it can be studied by using differential calculus. Lie demonstrated that an nth order ordinary differential equation which is invariant under a one-parameter group of point transformations may be constructively reduced to an ordinary differential equation of order (n - 1). When Lie's method is applied to a system of partial differential equations which are invariant under a Lie group of point transformations, one may constructively obtain solutions that are invariant under some subgroup or the entire group admitted by the system. Lie group analysis has its applications in a wide variety of fields such as algebraic topology, differential geometry, general relativity and numerical analysis, all of which are well covered in texts such as Anderson and Ibragimov (1979), Bluman and Kumei (1989) and Ibragimov (1995).

The structure of this chapter is as follows : in §3.2 we present a brief outline of conformal geometry relevant to this chapter. §3.3 begins with Lie group analysis and we obtain the Einstein field equations. In §3.4 and §3.5 corrections are made to the paper by Hansraj *et al* (2013) which appears in this chapter, and we construct static and nonstatic solutions respectively. Our solutions are tested for physical plausibility with the aid of graphical plots. We present a spacetime foliation in §3.6 and the chapter is concluded in §3.7 with a discussion of our findings.

3.2 Conformal Geometry

In chapter 2 we presented the mathematical framework for general relativity by outlining the concepts in differential geometry. This chapter requires, in addition to differential geometry, a few aspects relating to conformal geometry and Lie analysis, which we provide a brief overview of in this section.

The commutator or Lie bracket for two first order linear differential operators $\mathbf{X}$ and

$\mathbf{Y}$ is defined as

$$[\mathbf{X}, \mathbf{Y}] = \mathbf{XY} - \mathbf{YX} \tag{3.2.1}$$

A Lie algebra is a finite dimensional vector space $\mathbf{V}$ having the bilinear product $[\mathbf{X}, \mathbf{Y}]$ as defined in 3.2.1 above. It is skew-symmetric. That is, $[\mathbf{X}, \mathbf{Y}] = -[\mathbf{Y}, \mathbf{X}]$, and satisfies the Jacobi identity $[\mathbf{X}, [\mathbf{Y}, \mathbf{Z}]] + [\mathbf{Y}, [\mathbf{Z}, \mathbf{X}]] + [\mathbf{Z}, [\mathbf{X}, \mathbf{Y}]] = 0$ for all $\mathbf{X}, \mathbf{Y}, \mathbf{Z} \in \mathbf{V}$.
The Lie bracket is related to the Lie derivative by the identities

$$\begin{aligned} \mathcal{L}_{\mathbf{X}} &= [\mathbf{X}, \mathbf{Y}] \\ \mathcal{L}_{[\mathbf{X},\mathbf{Y}]} &= [\mathcal{L}_{\mathbf{X}}, \mathcal{L}_{\mathbf{Y}}] \end{aligned}$$

for vector fields $\mathbf{X}$ and $\mathbf{Y}$. There exists a close relationship between Lie algebras and Lie groups : every Lie algebra defines a unique simply connected Lie group. The properties of a Lie group are largely determined by those of its associated Lie algebra. A variety of symmetries may be defined on the manifold by the action of $\mathcal{L}_{\mathbf{X}}$ on the metric tensor and associated quantities, as illustrated in Katzin *et al* (1969) and Katzin and Levine (1972). Of the various symmetries that are possible, we are primarily concerned with conformal motions. A conformal Killing vector $\mathbf{X}$ is defined by the action of $\mathcal{L}_{\mathbf{X}}$ on the metric tensor field $\mathbf{g}$ so that

$$\mathcal{L}_{\mathbf{X}} g_{ab} = 2\psi g_{ab} \tag{3.2.2}$$

where $\psi(x^a)$ is the conformal factor.
There are four special cases associated with (3.2.2), and these are illustrated in the table that follows.

1. $\psi = 0$	$\mathbf{X}$ is a Killing vector
2. $\psi_{;a} = 0 \neq \psi$	$\mathbf{X}$ is a homothetic Killing vector
3. $\psi_{;ab} = 0 \neq \psi_{;a}$	$\mathbf{X}$ is a special conformal Killing vector
4. $\psi_{;ab} \neq 0$	$\mathbf{X}$ is a nonspecial conformal Killing vector

The spanning set $\{\mathbf{X}_A\} = \{\mathbf{X}_1, \mathbf{X}_2, ...\mathbf{X}_r\}$ of all the conformal Killing vectors of a spacetime generates a Lie algebra. The elements of this basis are related by

$$\begin{aligned}[\mathbf{X}_A, \mathbf{X}_B] &= \mathbf{X}_A\mathbf{X}_B - \mathbf{X}_B\mathbf{X}_A \\ &= C^D{}_{AB}\mathbf{X}_D\end{aligned}$$

where the quantities $C^D{}_{AB}$ are the structure constants of the group. The structure constants have the property of being independent of the coordinate system but do depend on the choice of the basis. The structure constants are skew–symmetric so that

$$C^D{}_{AB} = -C^D{}_{BA}$$

and satisfy the identity

$$C^E{}_{AD}C^D{}_{BC} + C^E{}_{BD}C^D{}_{CA} + C^E{}_{CD}C^D{}_{AB} = 0.$$

The integrability condition for the existence of a conformal symmetry is given by

$$\mathcal{L}_{\mathbf{X}}C^a{}_{bcd} = 0 \qquad (3.2.3)$$

Suppose that we are given a spacetime $(M, \mathbf{g})$ with line element

$$ds^2 = g_{ab}dx^a dx^b \tag{3.2.4}$$

and a related spacetime $(M, \bar{\mathbf{g}})$ with the line element

$$d\bar{s}^2 = \bar{g}_{ab}dx^a dx^b \tag{3.2.5}$$

Then (3.2.4) and (3.2.5) are said to be conformally related if

$$\bar{g}_{ab} = e^{2U} g_{ab} \ \text{ and } \ \bar{g}^{ab} = e^{-2U} g^{ab} \tag{3.2.6}$$

where $U(x^c)$ is a nonzero, real–valued function of the coordinates on M. This transformation between $\bar{\mathbf{g}}$ and $\mathbf{g}$ is called a conformal transformation and is a special type of mapping between metric spaces given by dilatation (or contraction) of all lengths by a common factor which varies from point to point.

The connection coefficients, Riemann curvature tensor, Ricci tensor and Ricci scalar for the metric g_{ab} are related to those of the metric $\bar{g}_{ab} = e^{2U} g_{ab}$ by the following formulae which are given in de Felice and Clarke (1990):

$$\bar{\Gamma}^a{}_{bc} = \Gamma^a_{bc} + \frac{1}{2}\left[\delta^a_b \phi_c + \delta^a_c \phi_b - g_{bc}\phi^a\right] \tag{3.2.7}$$

$$\begin{aligned} \bar{R}^a{}_{bcd} &= R^a{}_{bcd} + \delta^a_{[d}\nabla_{c]}\phi_b + g_{b[c}\nabla_{d]}\phi^a \\ &\quad + \frac{1}{2}\delta^a{}_{[c}\phi_{d]}\phi_b - \frac{1}{2}g_{b[c}\phi_{d]}\phi^a - \frac{1}{2}\delta^a{}_{[c}g_{d]b}\phi^e\phi_e \end{aligned} \tag{3.2.8}$$

$$\bar{R}_{bd} = R_{bd} - \frac{1}{2}\left[2\phi_{b;d} - \phi_a\phi_b + g_{ab}\phi^e\phi_e\right] - \frac{1}{2}g_{bd}\phi^a{}_{;a} \tag{3.2.9}$$

$$\bar{R} = \frac{1}{\Omega}\left[R - 3\phi^e{}_{;e} - \frac{3}{2}\phi_e\phi^e\right] \tag{3.2.10}$$

where we have defined $\phi_a = \partial_a(\ln\Omega)$ and $\Omega = e^{2U}$. Additionally the conformal Einstein tensor $\bar{\mathbf{G}}$ is given by

$$\bar{G}_{ab} = G_{ab} + 2\left(U_a U_b - \frac{1}{2}U^c U_c g_{ab}\right) + 2(U^c{}_{;c} + U^c U_c)g_{ab} - 2U_{a;b} \tag{3.2.11}$$

where the covariant derivatives and contractions are calculated on the original metric g_{ab}.

3.3 Einstein Field Equations

We consider the metric

$$ds^2 = -dt^2 + dx^2 + e^{2\nu(y,z)}(dy^2 + dz^2) \tag{3.3.1}$$

which, according to Petrov classification (1954), is of type D. A solution of (3.2.2) for the given metric reveals that (3.3.1) admits three Killing vectors, namely

$$\begin{aligned} X_1 &= \partial_t \\ X_2 &= \partial_x \\ X_3 &= x\,\partial_t + t\,\partial_x \end{aligned}$$

with the Lie bracket relations

$$\begin{aligned} [X_1,\ X_2] &= 0 \\ [X_1,\ X_3] &= X_2 \\ [X_2,\ X_3] &= X_1. \end{aligned}$$

The conformally related analogue is given by

$$ds^2 = e^{2U(t,x,y,z)}\left[-dt^2 + dx^2 + e^{2\nu(y,z)}(dy^2 + dz^2)\right]. \tag{3.3.2}$$

By the Defrise-Carter (1975) theorem, the Killing vectors above are now conformal Killing vectors, given by

$$\begin{aligned} Y_1 &= U_t \\ Y_2 &= U_x \\ Y_3 &= x\,U_t + t\,U_x. \end{aligned}$$

Note that the expression $\nu_{yy} + \nu_{zz}$ is nonzero. If this expression was zero, the Weyl tensor would vanish leading to conformally flat solutions. Such solutions have already been fully determined as Stephani (1967) stars in the case of expansion or generalised Schwarzschild metrics for no expansion.

To determine the perfect fluid energy–momentum tensor, we select a fluid 4–velocity vector **u** that is non-comoving of the form

$$u^a = e^{-U} \left(\cosh v \delta^a_0 + \sinh v \delta^a_1 \right)$$

where $v = v(t, x)$. Note that utilising a comoving velocity field would also lead to conformal flatness and this case is not of immense interest as explained above.

For the line element (3.3.2), the coupling of the conformal Einstein tensor and the transformed energy momentum tensor yields the Einstein field equations, given by

$$U_t U_y - U_{ty} = 0 \tag{3.3.3}$$

$$U_t U_z - U_{tz} = 0 \tag{3.3.4}$$

$$U_x U_y - U_{xy} = 0 \tag{3.3.5}$$

$$U_x U_z - U_{xz} = 0 \tag{3.3.6}$$

$$U_t U_x - U_{tx} = -\frac{1}{4}(\mu + p)e^{2U} \sinh 2v \tag{3.3.7}$$

$$U_y U_z - U_{yz} + \nu_z U_y + \nu_y U_z = 0 \tag{3.3.8}$$

$$\begin{aligned} &-2U_{xx} - U_x^2 + 3U_t^2 \\ &-e^{-2\nu}\left(2U_{yy} + 2U_{zz} + U_y^2 + U_z^2 + \nu_{yy} + \nu_{zz}\right) = \left((\mu + p)\cosh^2 v - p\right) e^{2U} \end{aligned} \tag{3.3.9}$$

$$\begin{aligned} &-2U_{tt} - U_t^2 + 3U_x^2 \\ &+e^{-2\nu}\left(2U_{yy} + 2U_{zz} + U_y^2 + U_z^2 + \nu_{yy} + \nu_{zz}\right) = \left((\mu + p)\sinh^2 v + p\right) e^{2U} \end{aligned} \tag{3.3.10}$$

$$\begin{aligned} &2U_{zz} + U_z^2 + 3U_y^2 + 2\nu_y U_y - 2\nu_z U_z \\ &+e^{2\nu}\left(2U_{xx} - 2U_{tt} + U_x^2 - U_t^2\right) = pe^{2\nu + 2U} \end{aligned} \tag{3.3.11}$$

$$\begin{aligned} &2U_{yy} + U_y^2 + 3U_z^2 - 2\nu_y U_y + 2\nu_z U_z \\ &+e^{2\nu}\left(2U_{xx} - 2U_{tt} + U_x^2 - U_t^2\right) = pe^{2\nu + 2U} \end{aligned} \tag{3.3.12}$$

The field equations may be reduced to a simpler form by observing that an immediate consequence of equations (3.3.3)–(3.3.6) is the functional form

$$e^{-U} = f(t, x) + h(y, z) \tag{3.3.13}$$

where f and h are arbitrary functions and $U = U(t, x, y, z)$. After a marathon of calculations it may be shown that equations (3.3.3) - (3.3.12) reduce to the simpler set of equations:

$$\mu = 3(f_t^2 - f_x^2) + (f+h)(4kf - 2kh + 3\alpha) - 3e^{-2\nu}\left(h_y^2 + h_z^2\right) \tag{3.3.14}$$

$$\begin{aligned} p = & -3(f_t^2 - f_x^2) \\ & +(f+h)\left(2f_{tt} - 2f_{xx} + 2kh - \alpha\right) + 3e^{-2\nu}\left(h_y^2 + h_z^2\right) \end{aligned} \tag{3.3.15}$$

$$\tanh^2 v = \frac{2f_{xx} - 2kf - \alpha}{2f_{tt} + 2kf + \alpha} \tag{3.3.16}$$

$$f_{tx}^2 = \frac{1}{4}\left(2f_{xx} - 2kf - \alpha\right)\left(2f_{tt} + 2kf + \alpha\right) \tag{3.3.17}$$

$$h_{yz} = \nu_z h_y + \nu_y h_z \tag{3.3.18}$$

$$h_{yy} - h_{zz} = 2\nu_y h_y + 2\nu_z h_z \tag{3.3.19}$$

where α is a separation constant and we have set $\nu_{yy} + \nu_{zz} = -2ke^{2\nu}$, k being a constant. The set of equations (3.3.14) - (3.3.19) have been discussed in general by Govinder and Hansraj (2012) with the help of the Lie group analysis approach. New exact solutions were reported, however, the difficulty of working with such solutions is that they are 4-dimensional and therefore it is not transparent whether the solutions could represent physically acceptable matter configurations. For this reason we elect to study some physical properties by neglecting the y and z directional contributions. So we adopt the approach of Castejon-Amenedo and Coley (1992) and set $h = 0$.

3.4 The Static Case

We begin by analysing the behaviour of our model when it is time-independent. Hence we consider the conformal factor in the form $U = U(x)$. The system of field equations (3.3.14) - (3.3.19) reduces to

$$\mu = -3f_x^2 + f(4kf + 3\alpha) \tag{3.4.1}$$

$$p = 3f_x^2 - f\left(2f_{xx} + \alpha\right) \tag{3.4.2}$$

$$\tanh^2 v = \frac{2f_{xx} - 2kf - \alpha}{2kf + \alpha} \tag{3.4.3}$$

$$0 = \left(2f_{xx} - 2kf - \alpha\right)\left(2kf + \alpha\right) \tag{3.4.4}$$

where α is a separation constant and k an arbitrary constant. To determine a solution for (3.4.4), we consider each of the brackets in turn. From $2kf + \alpha = 0$ we obtain $f(x) = -\frac{\alpha}{2k}$ which produces the trivial solution of a constant conformal factor. We then consider the equation

$$2f_{xx} - 2kf - \alpha = 0 \tag{3.4.5}$$

This is a second order differential equation with constant coefficients, and its solution may be expressed in three categories as follows :

$$f(x) = \begin{cases} \frac{\alpha}{4}x^2 + C_1 x + C_2, & k = 0; \\ -\frac{\alpha}{2k} + C_1 \cos\sqrt{-k}x + C_2 \sin\sqrt{-k}x, & k < 0; \\ -\frac{\alpha}{2k} + C_1 \cosh\sqrt{k}x + C_2 \sinh\sqrt{k}x, & k > 0. \end{cases}$$

where C_1 and C_2 are constants of integration.

Note that in the work that follows, without loss of generality, the separation constant α is taken to be positive.

We now do an analysis of each of the three cases for k.

3.4.1 $k = 0$

For the case $k = 0$ we obtain the explicit forms for the kinematical and dynamical variables, so that the complete solution for the conformally related Einstein field equations may be given by

$$
\begin{aligned}
e^{-U(x)} &= \frac{\alpha}{4}x^2 + C_1 x + C_2 \\
\mu &= -3c_1^2 + 3\alpha c_2 \\
p &= \frac{1}{4}\alpha^2 x^2 + \alpha C_1 x + (3C_1^2 - 2\alpha C_2) \\
\tanh v &= 0
\end{aligned}
$$

This case is not physically interesting since $k = 0$ results in a metric that is conformally flat. Such solutions have been found up to integration in general. Note that the tilting angle ν vanishes, and this supports the conformal flatness of the spacetime geometry for which $k = 0$. Furthermore we observe that the solution produces a constant density, which is analogous to the Schwarzschild constant density solution. Subsequently the sound-speed index $\frac{dp}{d\mu}$ would be infinite. Hence we deduce that the solution for the static case $k = 0$ is unphysical.

3.4.2 $k < 0$

The energy density, pressure and sound-speed index are respectively given by

$$\mu = 3k\tilde{j}^2 + \left(\frac{-\alpha}{2k} + j\right)(\alpha + 4kj) \tag{3.4.6}$$

$$p = -3k\tilde{j}^2 - \left(\frac{-\alpha}{2k} + j\right)(\alpha + 2kj) \tag{3.4.7}$$

$$\frac{dp}{d\mu} = \frac{2kj}{2kj - \alpha} \tag{3.4.8}$$

where we have defined $j = C_1 \cos\sqrt{-k}x + C_2 \sin\sqrt{-k}x$ and
$\tilde{j} = C_2 \cos\sqrt{-k}x - C_1 \sin\sqrt{-k}x$.

In order to satisfy the weak, strong and dominant energy conditions, it is required that each of $\mu - p$, $\mu + p$ and $\mu + 3p$ be positive. So we determine the expressions for these three quantities which are given by

$$\mu - p = 6k\tilde{j}^2 + \frac{(-\alpha + 2kj)(\alpha + 3kj)}{k} \tag{3.4.9}$$

$$\mu + p = \frac{kj(-\alpha + kj)}{k} \tag{3.4.10}$$

$$\mu + 3p = -6k\tilde{j}^2 - \frac{(-\alpha + 2kj)(\alpha + kj)}{k} \tag{3.4.11}$$

We must now select suitable values for each of the constants k, α, C_1 and C_2 in order to obtain solutions which could potentially be used to generate physically realistic astrophysical models. To attempt going forward in a random manner could prove to be a lengthy and possibly unsuccessful task. So, in order to reduce the arbitrariness in choosing these constants, we proceed in a more systematic manner. We begin by considering the behaviour of the dynamical variables at the central axis corresponding to $x = 0$, since the constants should be compatible with a regular centre in the first place. We use the subscript 0 to denote the quantities (3.4.6) - (3.4.8) at the centre.

Also note that when $x = 0$, then $j = C_1$ and $\tilde{j} = C_2$. So we obtain

$$\mu_0 = \frac{6k^2C_2^2 + 8k^2C_1^2 - 2\alpha kC_1 - \alpha^2}{2k} > 0 \tag{3.4.12}$$

$$p_0 = \frac{-6k^2C_2^2 - 4k^2C_1^2 + \alpha^2}{2k} \geq 0 \tag{3.4.13}$$

$$0 < \left(\frac{dp}{d\mu}\right)_0 = \frac{2kC_1}{2kC_1 - \alpha} < 1 \tag{3.4.14}$$

The right-most inequality of (3.4.14) simplifies to $\frac{\alpha}{2kC_1-\alpha} < 0$. Bearing in mind that, at the outset, we elected to have $\alpha > 0$, it follows that $2kC_1 - \alpha < 0$, from which we deduce that $C_1 < \frac{\alpha}{2k}$.

The left-most inequality of (3.4.14) tells us that $\frac{2kC_1}{2kC_1-\alpha}$ is positive. This leads to two possibilities for us to consider:

- Option 1

  $2kC_1 > 0$ and $2kC_1 - \alpha > 0$.

  These two conditions collectively prescribe that $C_1 < 0$ (since $k < 0$) and $C_1 > \frac{\alpha}{2k}$, which contradicts the right side of the inequality (3.4.14). Hence we disregard option 1.

- Option 2

  $2kC_1 < 0$ and $2kC_1 - \alpha < 0$.

  From these we have that $C_1 > 0$ and $C_1 < \frac{\alpha}{2k}$. However, the combination of $\alpha > 0$ and $k < 0$ infer that $\frac{\alpha}{2k} < 0$ which is a contradiction to our prior statement.

We do not pursue the case $k < 0$ any further as there is no possibility of producing a physically reasonable model.

3.4.3 $k > 0$

The energy density, pressure and sound–speed parameter have the forms

$$\mu = -3k\tilde{g}^2 + \left(\frac{-\alpha}{2k} + g\right)(\alpha + 4kg) \tag{3.4.15}$$

$$p = 3k\tilde{g}^2 - \left(\frac{-\alpha}{2k} + g\right)(\alpha + 2kg) \tag{3.4.16}$$

$$\frac{dp}{d\mu} = \frac{2kg}{2kg - \alpha} \tag{3.4.17}$$

respectively, where we have defined $g = C_1 \cosh\sqrt{k}x + C_2 \sinh\sqrt{k}x$ and $\tilde{g} = C_2 \cosh\sqrt{k}x + C_1 \sinh\sqrt{k}x$.

We again determine the weak, strong and dominant energy conditions, which are given by

$$\mu - p = -6k\tilde{g}^2 + 2\left(\frac{-\alpha}{2k} + g\right)(\alpha + 3kg) \tag{3.4.18}$$

$$\mu + p = 2kg\left(\frac{-\alpha}{2k} + g\right) \tag{3.4.19}$$

$$\mu + 3p = 6k\tilde{g}^2 + \frac{(\alpha + kg)(\alpha - 2kg)}{k} \tag{3.4.20}$$

Once more we analyse the behaviour of the dynamical variables at the central axis corresponding to $x = 0$. Using the subscript 0 to denote the quantities (3.4.15) - (3.4.17) at the centre and bearing in mind that when $x = 0$, then $g = C_1$ and $\tilde{g} = C_2$, we obtain

$$\mu_0 = \frac{-6k^2C_2^2 + 8k^2C_1^2 - 2\alpha kC_1 - \alpha^2}{2k} \geq 0 \tag{3.4.21}$$

$$p_0 = \frac{6k^2C_2^2 - 4k^2C_1^2 + \alpha^2}{2k} \geq 0 \tag{3.4.22}$$

$$0 < \left(\frac{dp}{d\mu}\right)_0 = \frac{2kC_1}{2kC_1 - \alpha} < 1 \tag{3.4.23}$$

The right-most inequality of (3.4.23) simplifies to $\frac{\alpha}{2kC_1-\alpha} < 0$. Since $\alpha > 0$, it follows that $2kC_1 - \alpha < 0$, from which we deduce that $C_1 < \frac{\alpha}{2k}$.

The left-most inequality of (3.4.23) tells us that $\frac{2kC_1}{2kC_1-\alpha}$ is positive. This again leads to two possibilities for us to consider:

- Option 1

  $2kC_1 > 0$ and $2kC_1 - \alpha > 0$.

  These two conditions infer that $C_1 > 0$ (since $k > 0$) and $C_1 > \frac{\alpha}{2k}$, which contradicts the right side of the inequality (3.4.23). Hence we do not consider option 1.

- Option 2

  $2kC_1 < 0$ and $2kC_1 - \alpha < 0$.

  From these we have that $C_1 < 0$ and $C_1 < \frac{\alpha}{2k}$, which is in agreement with the right side of (3.4.23).

We are now in a position to narrow down our choices as follows : $k > 0$, $\alpha > 0$, $C_1 < 0$ with $C_1 < \frac{\alpha}{2k}$. Additionally, combining (3.4.21) and (3.4.22) produces the inequality $4k^2C_1^2 - \alpha^2 \leq 6k^2C_2^2 \leq 8k^2C_1^2 - 2\alpha kC_1 - \alpha^2$, and we note that our choice for C_2 is constrained by the values we select for k, α and C_1.
Empirical testing results in the following set of values which satisfy the relevant conditions : $k = 1$, $\alpha = 2$, $C_1 = -2.4$ and $C_2 = 2.153$.

We generate the relevant plots for our chosen values, and analyse our solution by examining Figure 3.1 - Figure 3.5.
From Figure 3.1, it is observed that the energy density is positive definite and monotonically decreasing throughout the interior of the fluid.
Figure 3.2 shows the pressure profile of our solution, and it is pleasing to note that the pressure is also positive and displays monotone decrease throughout. An important characteristic of Figure 3.2 is that the pressure vanishes at $x = 1$, demonstrating the

possibility of a pressure-free hypersurface which defines the boundary for the matter distribution.

Figure 3.3 illustrates the adiabatic sound-speed index $\frac{dp}{d\mu}$ which is positive, monotonically decreasing and lies between 0 and 1 throughout the interior of the spacetime. This indicates that the causal requirement is satisfied. That is, the speed of sound does not exceed the speed of light.

Figure 3.4 illustrates the positivity of $\mu - p$, $\mu + p$ and $\mu + 3p$, thereby confirming that the weak, strong and dominant energy conditions are satisfied throughout the fluid.

Figures 3.1 - 3.4 reveal that our solution for $k > 0$ satisfies the relevant conditions and shows potential for modeling acceptable astrophysical phenomena.

In modeling of astrophysical objects such as stars, the stability of the star is an important criterion. We investigate the stability of our solution by employing the Chandrasekar stability index which is given by

$$\Gamma = \frac{\mu + p}{p}\frac{dp}{d\mu} \tag{3.4.24}$$

In order for the configuration to be stable, it is required that $\Gamma > \frac{4}{3}$.

Figure 3.5 shows the graphs of $\Gamma = \frac{\mu+p}{p}\frac{dp}{d\mu}$ for the interval $x = 0$ to $x = 1$, and $\Gamma = \frac{4}{3}$ on the same set of axes. It is a pleasing feature of the plots that the stability function lies above the line $\frac{4}{3}$, confirming that the stability condition is satisfied.

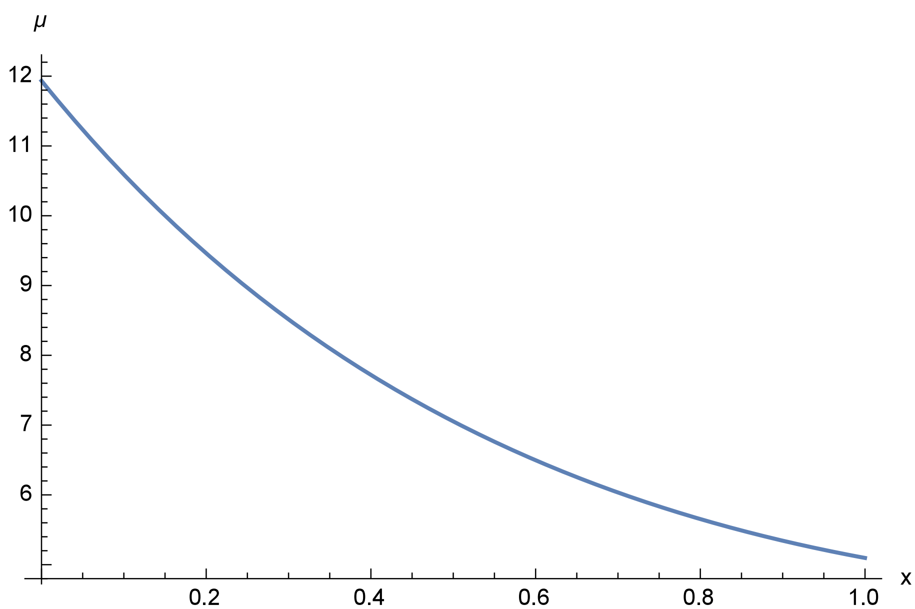

Figure 3.1: Energy density (μ) as a function of x for the static case $k > 0$ using the values $k = 1$, $\alpha = 2$, $C_1 = -2.4$ and $C_2 = 2.153$

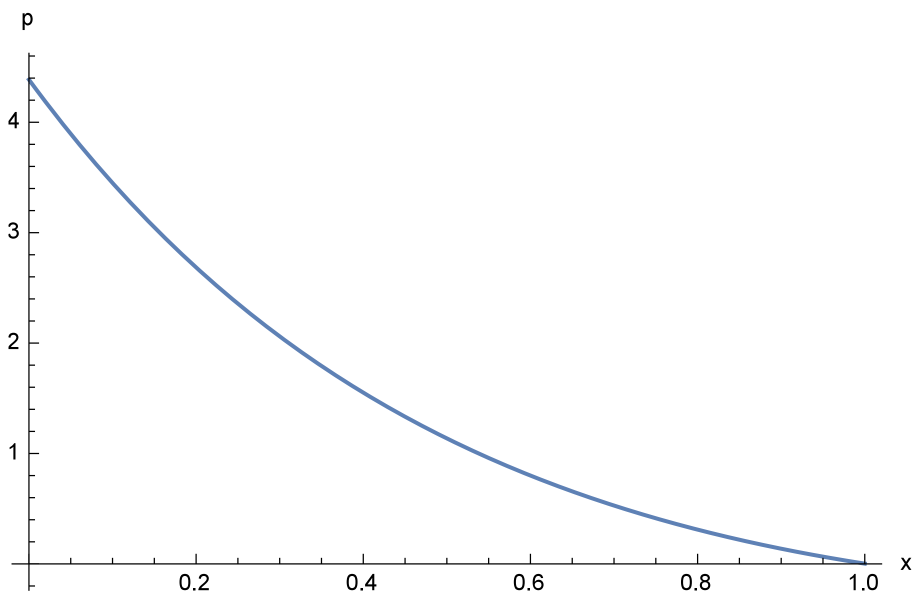

Figure 3.2: Pressure (p) as a function of x for the static case $k > 0$ using the values $k = 1$, $\alpha = 2$, $C_1 = -2.4$ and $C_2 = 2.153$

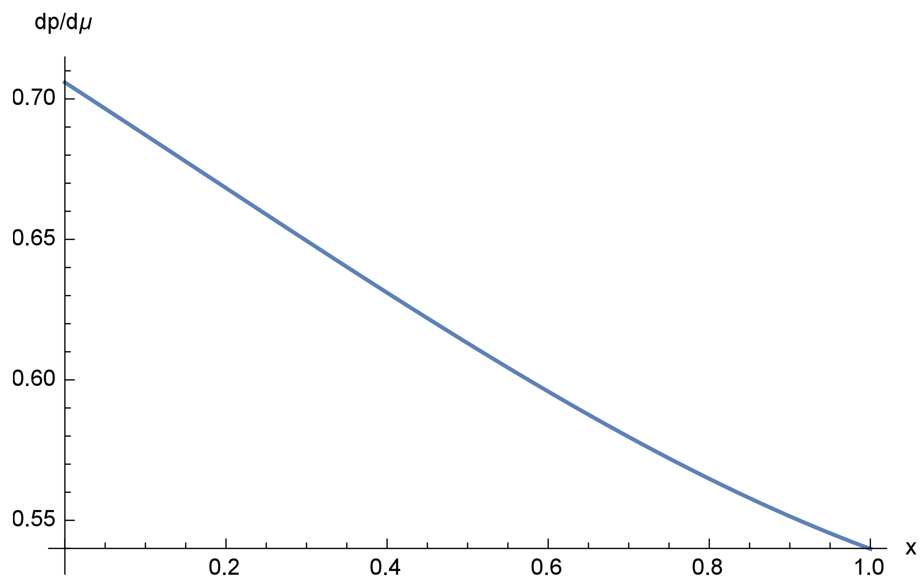

Figure 3.3: Sound-speed $(\frac{dp}{d\mu})$ as a function of x for the static case $k > 0$ using the values $k = 1$, $\alpha = 2$, $C_1 = -2.4$ and $C_2 = 2.153$

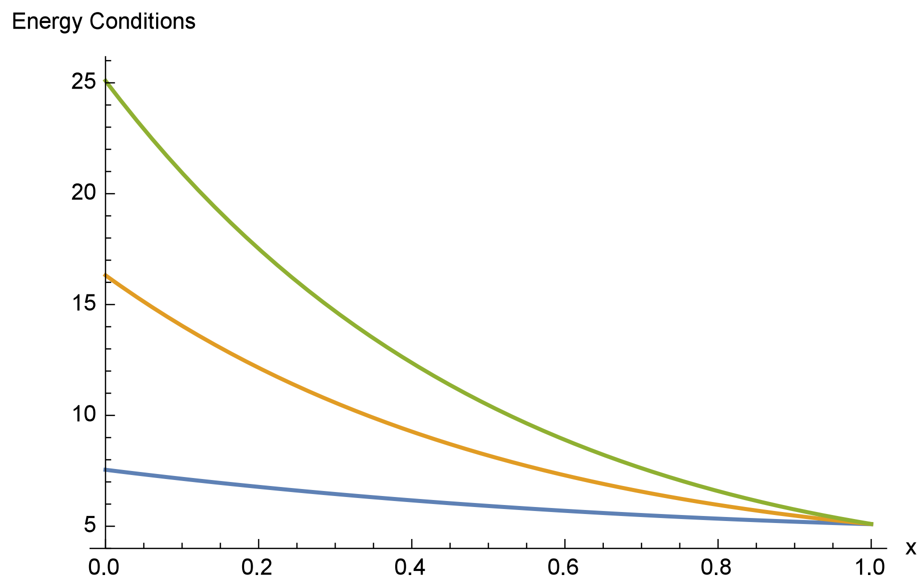

Figure 3.4: Energy conditions $\mu - p$ (blue), $\mu + p$ (yellow) and $\mu + 3p$ (green) as functions of x for the static case $k > 0$ using the values $k = 1$, $\alpha = 2$, $C_1 = -2.4$ and $C_2 = 2.153$

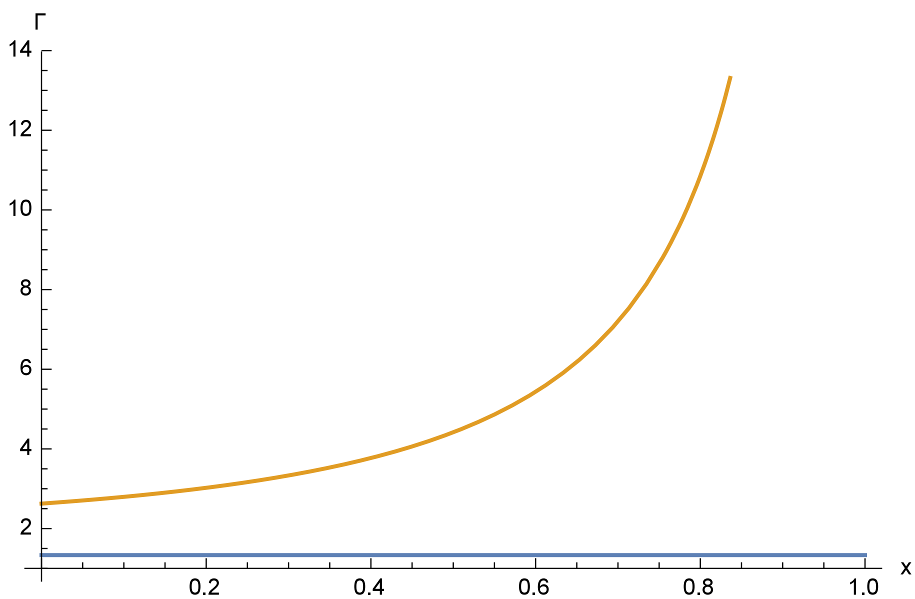

Figure 3.5: Stability factor Γ (yellow) as a function of x for the static case $k > 0$ using the values $k = 1$, $\alpha = 2$, $C_1 = -2.4$ and $C_2 = 2.153$

3.5 The Nonstatic Case

Finding nonstatic exact solutions of the Einstein equations for a particular configuration of matter is non-trivial. The method of conformal transformations affords us a means to construct nonstatic solutions from known static metrics. In the case under investigation we suppose that the conformal factor has the simple form $U = U(t)$. The field equations then have the familiar form

$$\mu = 3f_t^2 + f(4kf + 3\alpha) \tag{3.5.1}$$

$$p = -3f_t^2 + f(2f_{tt} - \alpha) \tag{3.5.2}$$

$$\tanh^2 v = \frac{-(2kf + \alpha)}{2f_{tt} + 2kf + \alpha} \tag{3.5.3}$$

$$0 = (2kf + \alpha)(2f_{tt} + 2kf + \alpha) \tag{3.5.4}$$

where we now have $f = f(t)$ only. Once again the conclusion $f(t) = -\frac{\alpha}{2k}$ leads to a trivial constant conformal factor so we do not pursue it further. Instead we again examine the other possibility more closely. That is, we solve the second order differential equation

$$2f_{tt} + 2kf + \alpha = 0 \tag{3.5.5}$$

to obtain

$$f(t) = \begin{cases} -\frac{\alpha}{4}t^2 + C_1 t + C_2, & k = 0; \\ -\frac{\alpha}{2k} + C_1 \cosh\sqrt{-k}t + C_2 \sinh\sqrt{-k}t, & k < 0; \\ -\frac{\alpha}{2k} + C_1 \cos\sqrt{k}t + C_2 \sin\sqrt{k}t, & k > 0. \end{cases}$$

where C_1 and C_2 are integration constants. As with the static case, we examine each of the three solutions in turn to see if any of them will lead to viable solutions.

3.5.1 $k = 0$

This case degenerates into a conformally flat metric and so it is not worthy of further attention as such metrics have already been discovered.

3.5.2 $k < 0$

The energy density, pressure and sound-speed index are respectively given by

$$\mu = -3k\tilde{v}^2 + \left(\frac{-\alpha}{2k} + v\right)(\alpha + 4kv) \tag{3.5.6}$$

$$p = 3k\tilde{v}^2 - \left(\frac{-\alpha}{2k} + v\right)(-\alpha - 2kv) \tag{3.5.7}$$

$$\frac{dp}{d\mu} = \frac{2kv}{2kv - \alpha} \tag{3.5.8}$$

where we have defined $v = C_1 \cosh\sqrt{-k}t + C_2 \sinh\sqrt{-k}t$ and $\tilde{v} = C_2 \cosh\sqrt{-k}t - C_1 \sinh\sqrt{-k}t$.

We also expect all physical constraints to be satisfied at the initial condition $t = 0$. Denoting initial values with the subscript 0 we have that the following inequalities must be satisfied:

$$\mu_0 = \frac{-6k^2C_2^2 + 8k^2C_1^2 + 2\alpha k C_1 - \alpha^2}{2k} > 0 \tag{3.5.9}$$

$$p_0 = \frac{6k^2C_2^2 - 4k^2C_1^2 + \alpha^2}{2k} \geq 0 \tag{3.5.10}$$

$$0 < \left(\frac{dp}{d\mu}\right)_0 = \frac{2kC_1}{2kC_1 - \alpha} < 1 \tag{3.5.11}$$

The left-most inequality of (3.5.11) infers that $C_1 > 0$ and $C_1 < \frac{\alpha}{2k}$. From these two conditions arises a contradiction, since $\alpha > 0$ and $k < 0$ implies $\frac{\alpha}{2k} < 0$. Hence C_1 can never be less than $\frac{\alpha}{2k}$. We conclude that no viable nonstatic solution is possible from the case $k < 0$.

3.5.3 $k > 0$

The energy density, pressure and sound–speed parameter have the forms

$$\mu = 3k\tilde{l}^2 + \left(\frac{-\alpha}{2k} + l\right)(\alpha + 4kl) \tag{3.5.12}$$

$$p = -3k\tilde{l}^2 + \left(\frac{-\alpha}{2k} + l\right)(-\alpha + 2kl) \tag{3.5.13}$$

$$\frac{dp}{d\mu} = \frac{2kl}{2kl - \alpha} \tag{3.5.14}$$

respectively, where we have defined $l = C_1 \cos\sqrt{k}t + C_2 \sin\sqrt{k}t$ and $\tilde{l} = C_2 \cos\sqrt{k}t - C_1 \sin\sqrt{k}t$.

The weak, strong and dominant energy conditions are given by

$$\mu - p = 6k\tilde{l}^2 + 2\left(\frac{-\alpha}{2k} + l\right)(\alpha + 3kl) \tag{3.5.15}$$

$$\mu + p = 2kl\left(\frac{-\alpha}{2k} + l\right) \tag{3.5.16}$$

$$\mu + 3p = -6k\tilde{l}^2 + \frac{(\alpha + kl)(\alpha - 2kl)}{k} \tag{3.5.17}$$

As with the case $k < 0$, we examine the behaviour of the dynamical variables for the initial condition corresponding to $t = 0$. Using the subscript 0 to denote the quantities (3.5.12) - (3.5.14) at $t = 0$, we obtain

$$\mu_0 = \frac{6k^2C_2^2 + 8k^2C_1^2 - 2\alpha kC_1 - \alpha^2}{2k} > 0 \tag{3.5.18}$$

$$p_0 = \frac{-6k^2C_2^2 + 4k^2C_1^2 - 4\alpha kC_1 + \alpha^2}{2k} \geq 0 \tag{3.5.19}$$

$$0 < \left(\frac{dp}{d\mu}\right)_0 = \frac{2kC_1}{2kC_1 - \alpha} < 1 \tag{3.5.20}$$

The left-most inequality of (3.5.20) tells us that that $C_1 < 0$ and $C_1 < \frac{\alpha}{2k}$, with $\alpha > 0$ and $k > 0$. Furthermore, (3.5.18) and (3.5.19) leads to the inequality

$8k^2C_1^2 - 2\alpha kC_1 - \alpha^2 < 6k^2C_2^2 \leq 4k^2C_1^2 - 4\alpha kC_1 + \alpha^2$, which informs that C_2 is constrained by the values we choose for k, α and C_1. With this in mind, we take $k = 1$, $\alpha = 5$, $C_1 = -2.4$ and $C_2 = 0.01$.

Our solution is examined for physical reasonableness. Since the energy density and pressure, represented by equations (3.5.12) and (3.5.13) respectively, are independent of the spatial coordinate x we deduce that this is a fluid whose energy density and pressure are homogenous. It is clear from equations (3.5.12) and (3.5.13) that the fluid obeys a barotropic equation of state of the form $p = p(\mu)$. Figure 3.6 shows the sound-speed $\frac{dp}{d\mu}$ which lies between 0 and 1, thus affirming causality. In Figure 3.7 the weak, strong and dominant energy conditions are all shown to be positive. Figure 3.8 illustrates $\Gamma > \frac{4}{3}$, thereby confirming that we have a solution that could be used to genarate a stable configuration.

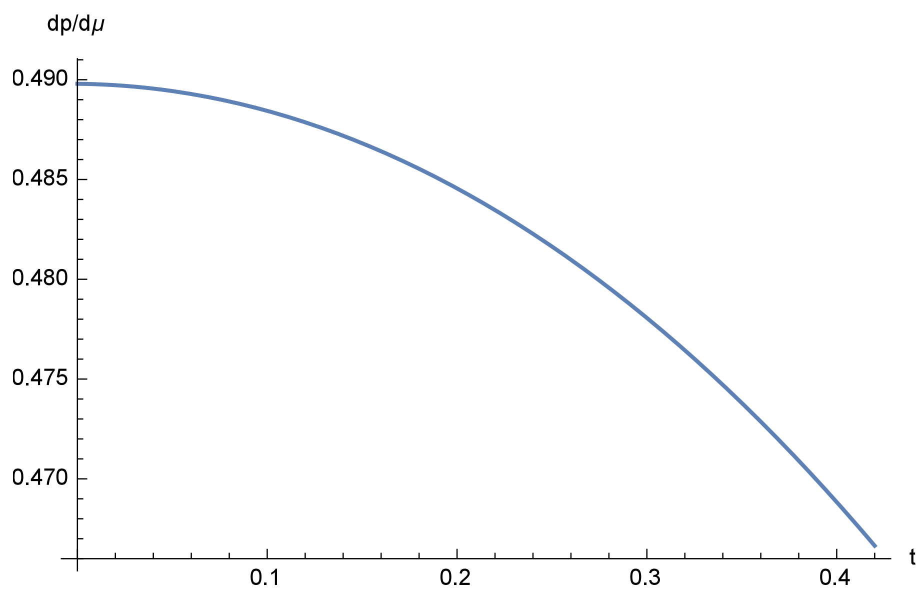

Figure 3.6: Sound-speed ($\frac{dp}{d\mu}$) as a function of t for the nonstatic case $k > 0$ using the values $k = 1$, $\alpha = 5$, $C_1 = -2.4$ and $C_2 = 0.01$

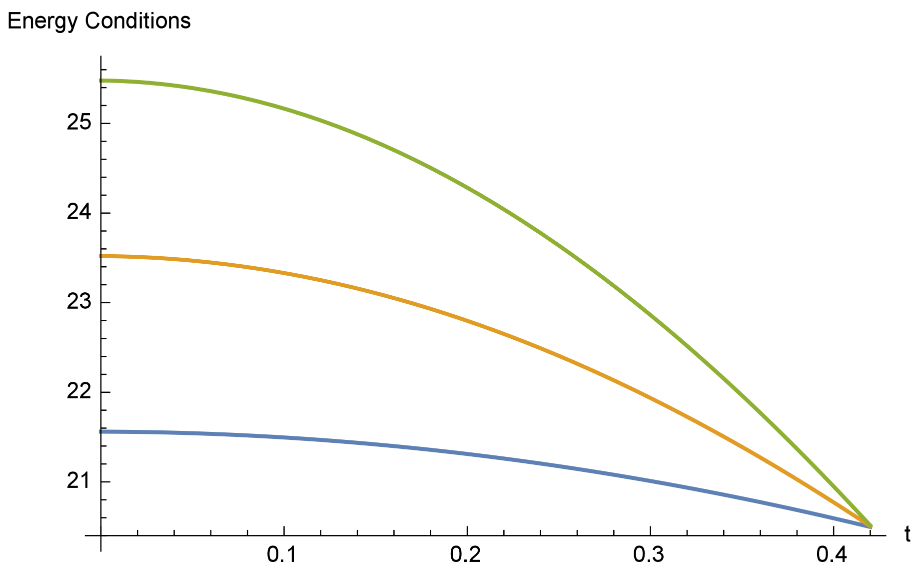

Figure 3.7: Energy conditions $\mu - p$ (blue), $\mu + p$ (yellow) and $\mu + 3p$ (green) as functions of t for the nonstatic case $k > 0$ using the values $k = 1$, $\alpha = 5$, $C_1 = -2.4$ and $C_2 = 0.01$

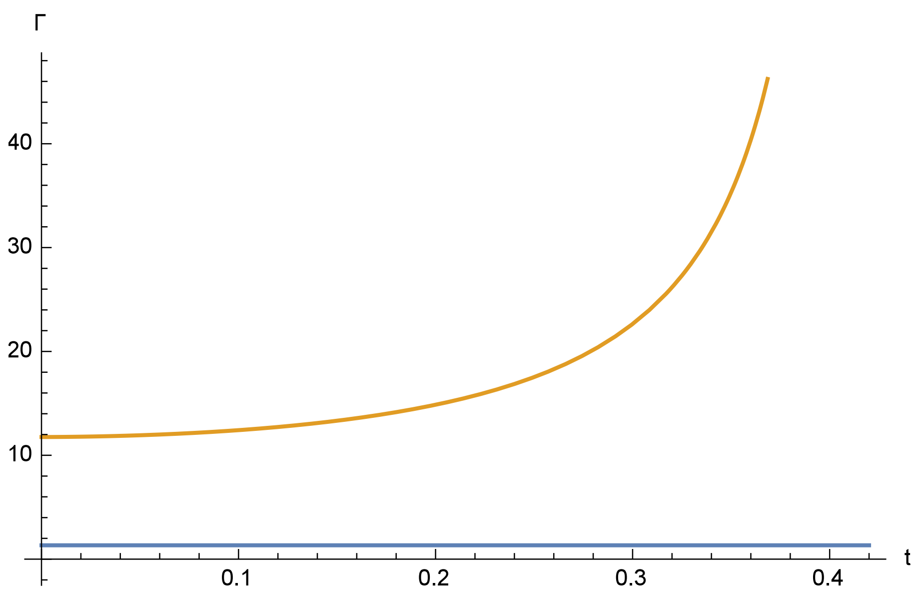

Figure 3.8: Stability factor Γ (yellow) as a function of t for the nonstatic case $k > 0$ using the values $k = 1$, $\alpha = 5$, $C_1 = -2.4$ and $C_2 = 0.01$

3.6 A Spacetime Foliation $U = U(t,x)$

The method of Lie group analysis has proved successful in generating broader classes of solutions than the ones discussed in §3.4 and §3.5. We turn our attention once more to the system of equations (3.3.14) - (3.3.19). The field equations (3.3.14) - (3.3.16) are taken as definitions for the energy density (μ), pressure (p) and the velocity vector angle (ν) respectively. Equation (3.3.17) depends only on f, where $f = f(t,x)$, for which solutions were obtained by Hansraj *et al* (2005). Implementing the method of Lie group analysis together with the aid of the computer package PROGRAM LIE, devised by Head (1993) equations (3.3.18) and (3.3.19) are solved to obtain

$$h(y,z) = z^{\frac{1}{4}} y^{\frac{3}{4}} e^{c_1 + \frac{z^2}{8y^2}} \tag{3.6.1}$$

$$\nu(y,z) = \frac{z^2}{16y^2} + \log\left[\left(\frac{z}{y}\right)^{\frac{3}{8}} \left(\frac{z^2}{y^2} - 1\right)^{\frac{1}{4}}\right] + c_2 \tag{3.6.2}$$

The functional form for $f(t,x)$, where $h = 0$, was given by Hansraj *et al* (2005)

$$f(t,x) = A \sinh\sqrt{k(t^2 - x^2)} + B\cosh\sqrt{k(t^2 - x^2)} \tag{3.6.3}$$

The solutions (3.6.1) - (3.6.3) are substituted into (3.3.2), and the conformally related metric may now be expressed as

$$ds^2 = \frac{-dt^2 + dx^2 + c_1 e^{\frac{z^2}{8y^2}} \left(\frac{z}{y}\right)^{\frac{3}{4}} \left(\frac{z^2}{y^2} - 1\right)^{\frac{1}{2}} (dy^2 + dz^2)}{\left(e^{c_1 + \frac{z^2}{8y^2}} y^{\frac{3}{4}} z^{\frac{1}{4}} + B\cosh\left[\sqrt{k(t^2 - x^2)}\right] + A\sinh\left[\sqrt{k(t^2 - x^2)}\right]\right)^2}$$

Now substituting the solutions for $f(t,x)$ and $h(y,z)$ into (3.3.14) and(3.3.15) yields the dynamical quantities μ and p, where

$$
\begin{aligned}
\mu \quad = \quad & -3\left(c_1 e^{\frac{z^2}{8y^2}}\left(\frac{z}{y}\right)^{\frac{3}{4}}\left(\frac{z^2}{y^2}-1\right)^{\frac{1}{2}}\right)^{-1} \\
& \left(\left(\frac{e^{c_1+\frac{z^2}{8y^2}}y^{\frac{3}{4}}}{4z^{\frac{3}{4}}}+\frac{e^{c_1+\frac{z^2}{8y^2}}z^{\frac{5}{4}}}{4y^{\frac{5}{4}}}\right)^2+\left(\frac{3e^{c_1+\frac{z^2}{8y^2}}z^{\frac{1}{4}}}{4y^{\frac{1}{4}}}-\frac{e^{c_1+\frac{z^2}{8y^2}}z^{\frac{9}{4}}}{4y^{\frac{9}{4}}}\right)^2\right) \\
& +\left(e^{c_1+\frac{z^2}{8y^2}}y^{\frac{3}{4}}z^{\frac{1}{4}}+B\cosh\left[\sqrt{k(t^2-x^2)}\right]+A\sinh\left[\sqrt{k(t^2-x^2)}\right]\right) \\
& \left(-2e^{c_1+\frac{z^2}{8y^2}}ky^{\frac{3}{4}}z^{\frac{1}{4}}-3\alpha+4k\left(B\cosh\left[\sqrt{k(t^2-x^2)}\right]+A\sinh\left[\sqrt{k(t^2-x^2)}\right]\right)\right) \\
& +3\left(\left(\frac{Akt\cosh\left[\sqrt{k(t^2-x^2)}\right]}{\sqrt{k(t^2-x^2)}}+\frac{Bkt\sinh\left[\sqrt{k(t^2-x^2)}\right]}{\sqrt{k(t^2-x^2)}}\right)^2\right. \\
& \left.-\left(-\frac{Akx\cosh\left[\sqrt{k(t^2-x^2)}\right]}{\sqrt{k(t^2-x^2)}}-\frac{Bkx\sinh\left[\sqrt{k(t^2-x^2)}\right]}{\sqrt{k(t^2-x^2)}}\right)^2\right) \quad ,
\end{aligned}
$$

and

$$
\begin{aligned}
p \;=\; & 3\left(c_1 e^{\frac{z^2}{8y^2}}\left(\frac{z}{y}\right)^{\frac{3}{4}}\left(\frac{z^2}{y^2}-1\right)^{\frac{1}{2}}\right)^{-1} \\
& \left(\left(\frac{e^{c_1+\frac{z^2}{8y^2}}y^{\frac{3}{4}}}{4z^{\frac{3}{4}}}+\frac{e^{c_1+\frac{z^2}{8y^2}}z^{\frac{5}{4}}}{4y^{\frac{5}{4}}}\right)^2+\left(\frac{3e^{c_1+\frac{z^2}{8y^2}}z^{\frac{1}{4}}}{4y^{\frac{1}{4}}}-\frac{e^{c_1+\frac{z^2}{8y^2}}z^{\frac{9}{4}}}{4y^{\frac{9}{4}}}\right)^2\right) \\
& -\frac{k(3t^2+x^2)}{t^2-x^2}\left(A\cosh\left[\sqrt{k(t^2-x^2)}\right]+B\sinh\left[\sqrt{k(t^2-x^2)}\right]\right)^2 \\
& +\left(e^{c_1+\frac{z^2}{8y^2}}y^{\frac{3}{4}}z^{\frac{1}{4}}+B\cosh\left[\sqrt{k(t^2-x^2)}\right]+A\sinh\left[\sqrt{k(t^2-x^2)}\right]\right)\left(-\alpha+2\left(e^{c_1+\frac{z^2}{8y^2}}ky^{\frac{3}{4}}z^{\frac{1}{4}}\right.\right. \\
& +A\left(-\frac{k^2t^2\cosh\left[\sqrt{k(t^2-x^2)}\right]}{(k(t^2-x^2))^{\frac{3}{2}}}+\frac{k\cosh\left[\sqrt{k(t^2-x^2)}\right]}{\sqrt{k(t^2-x^2)}}+\frac{kt^2\sinh\left[\sqrt{k(t^2-x^2)}\right]}{t^2-x^2}\right) \\
& -A\left(-\frac{k^2x^2\cosh\left[\sqrt{k(t^2-x^2)}\right]}{(k(t^2-x^2))^{\frac{3}{2}}}-\frac{k\cosh\left[\sqrt{k(t^2-x^2)}\right]}{\sqrt{k(t^2-x^2)}}+\frac{kx^2\sinh\left[\sqrt{k(t^2-x^2)}\right]}{t^2-x^2}\right) \\
& -B\left(\frac{kx^2\cosh\left[\sqrt{k(t^2-x^2)}\right]}{t^2-x^2}-\frac{k^2x^2\sinh\left[\sqrt{k(t^2-x^2)}\right]}{(k(t^2-x^2))^{\frac{3}{2}}}-\frac{k\sinh\left[\sqrt{k(t^2-x^2)}\right]}{\sqrt{k(t^2-x^2)}}\right) \\
& \left.\left.+B\left(-\frac{kt^2\cosh\left[\sqrt{k(t^2-x^2)}\right]}{t^2-x^2}-\frac{k^2t^2\sinh\left[\sqrt{k(t^2-x^2)}\right]}{(k(t^2-x^2))^{\frac{3}{2}}}+\frac{k\sinh\left[\sqrt{k(t^2-x^2)}\right]}{\sqrt{k(t^2-x^2)}}\right)\right)\right)\right).
\end{aligned}
$$

To analyse the pressure and density profiles with rigour when they are expressed in terms of all four variables t, x, y and z is not possible in view of the complexity of the expressions that μ and p are represented by. Even a graphical representation of the 4-dimensional solution is not possible. Hence, we consider a simplified solution in the form of a foliation of the distribution, which is expressed in terms of the temporal coordinate and one spatial coordinate. We accordingly select the particular solution $f(t,x)$ as expressed in equation (3.6.3). For this solution, the energy density and pressure respectively simplify to

$$\mu = 4k\left(B\cosh\left[\sqrt{k(t^2-x^2)}\right] + A\sinh\left[\sqrt{k(t^2-x^2)}\right]\right)^2$$

$$-3\left(\left(\frac{Akt\cosh\left[\sqrt{k(t^2-x^2)}\right]}{\sqrt{k(t^2-x^2)}} + \frac{Bkt\sinh\left[\sqrt{k(t^2-x^2)}\right]}{\sqrt{k(t^2-x^2)}}\right)^2\right.$$

$$\left.-\left(-\frac{Akx\cosh\left[\sqrt{k(t^2-x^2)}\right]}{\sqrt{k(t^2-x^2)}} - \frac{Bkx\sinh\left[\sqrt{k(t^2-x^2)}\right]}{\sqrt{k(t^2-x^2)}}\right)^2\right)$$

and

$$p = 2\left(B\cosh\left[\sqrt{k(t^2-x^2)}\right] + A\sinh\left[\sqrt{k(t^2-x^2)}\right]\right)$$

$$\left(A\left(-\frac{k^2t^2\cosh\left[\sqrt{k(t^2-x^2)}\right]}{(k(t^2-x^2))^{3/2}} + \frac{k\cosh\left[\sqrt{k(t^2-x^2)}\right]}{\sqrt{k(t^2-x^2)}} + \frac{kt^2\sinh\left[\sqrt{k(t^2-x^2)}\right]}{t^2-x^2}\right)\right.$$

$$-A\left(-\frac{k^2x^2\cosh\left[\sqrt{k(t^2-x^2)}\right]}{(k(t^2-x^2))^{3/2}} - \frac{k\cosh\left[\sqrt{k(t^2-x^2)}\right]}{\sqrt{k(t^2-x^2)}} + \frac{kx^2\sinh\left[\sqrt{k(t^2-x^2)}\right]}{t^2-x^2}\right)$$

$$-B\left(\frac{kx^2\cosh\left[\sqrt{k(t^2-x^2)}\right]}{t^2-x^2} - \frac{k^2x^2\sinh\left[\sqrt{k(t^2-x^2)}\right]}{(k(t^2-x^2))^{3/2}} - \frac{k\sinh\left[\sqrt{k(t^2-x^2)}\right]}{\sqrt{k(t^2-x^2)}}\right)$$

$$\left.+B\left(\frac{kt^2\cosh\left[\sqrt{k(t^2-x^2)}\right]}{t^2-x^2} - \frac{k^2t^2\sinh\left[\sqrt{k(t^2-x^2)}\right]}{(k(t^2-x^2))^{3/2}} + \frac{k\sinh\left[\sqrt{k(t^2-x^2)}\right]}{\sqrt{k(t^2-x^2)}}\right)\right)$$

$$-\frac{k(3t^2+x^2)}{t^2-x^2)}\left(A\cosh\left[\sqrt{k(t^2-x^2)}\right] + B\sinh\left[\sqrt{k(t^2-x^2)}\right]\right)^2.$$

In order to obtain an indication of the model's feasibility to represent a realistic distribution, we elect to make a graphical study of this solution. We must select appropriate values for the parameters A, B and k in order to finalise the model. Taking $A = 1$, $B = 10$ and $k = 0.1$ we are able to generate plots of the energy density (Figure 3.9) and pressure (Figure 3.10), both of which demonstrate pleasing features. For example, it is evident that in the region chosen, the energy density and pressure are both positive.

These are the most basic requirements for models to serve as candidates for realistic celestial phenomena. Therefore it is possible that this solution could be used to model a realistic configuration of a perfect fluid.

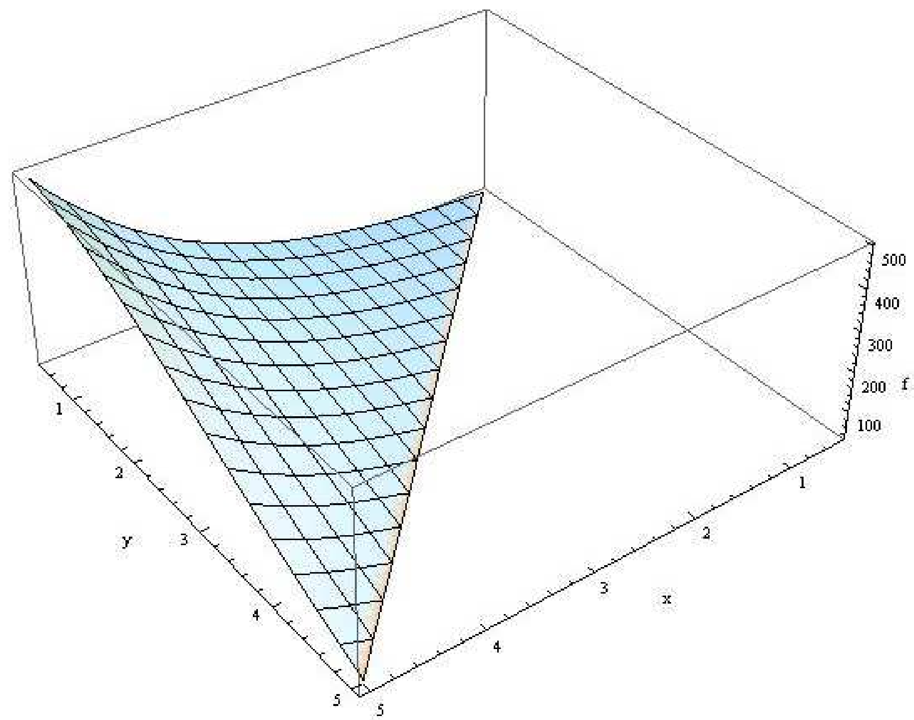

Figure 3.9: Energy density (μ) as a function of t and x using the values $A = 1$, $B = 10$ and $k = 0.1$

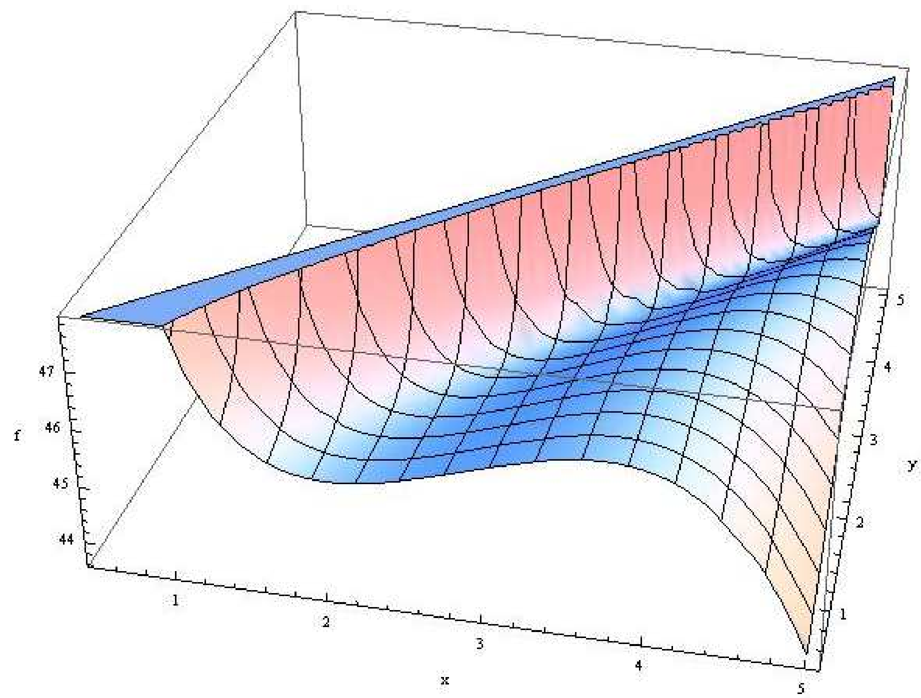

Figure 3.10: Pressure (p) as a function of t and x using the values $A = 1$, $B = 10$ and $k = 0.1$

3.7 Discussion

In this chapter, we have demonstrated that that new static and nonstatic solutions of the Einstein field equations may be constructed from known solutions through the use of conformal mappings. The reason for the success of this method is that the seed solution is already a solution of the (possibly vacuum) Einstein field equations. The Einstein tensor splits up neatly into a part containing the original Einstein tensor, and an expression involving the conformal factor. It is this latter part that must be coupled with an appropriate perfect fluid. We endeavoured to construct explicit solutions by considering cases where the conformal factor is a function of a space variable $U(x)$, a function of the temporal coordinate $U(t)$ and finally the case of a conformal factor as a function of space and time $U = U(t, x)$. An analysis of the first two of these cases through graphical plots showed that both solutions displayed pleasing behaviour. In both of the cases $U = U(x)$ and $U = U(t)$, it was possible to show the positivity of pressure and energy density, vanishing of pressure at a finite boundary, monotonic decrease of pressure and density to a finite boundary and subluminal sound- speed. We were able to further show, with the aid of the Chandrasekhar stability index, that the condition of stability was satisfied. The third case where $U = U(t, x)$ demonstrated the most basic requirement of positive pressure and energy density. We have therefore succeeded in obtaining solutions through the method of conformal mappings which could possibly generate physically acceptable models.

Chapter 4

Plane Symmetric Perfect Fluids

4.1 Introduction

Plane symmetric perfect fluid distributions were first discussed by Taub in 1951. The most general form of the metric for a plane symmetric spacetime, in Cartesian coordinates, is given by

$$ds^2 = A^2(dt^2 - dx^2) - B^2dy^2 - C^2dz^2$$

where the metric potentials A, B and C are functions of the spacetime variables x and t.

Plane symmetric spacetimes admit a three-parameter group of motions in the Euclidean plane. Taub (1951) demonstrated that spacetimes which possess plane symmetry have properties similar to those of spherically symmetric spacetimes. The Friedmann-Lemaître-Robertson-Walker (FLRW) cosmological model is viewed as an acceptable model of the universe. Amongst the assumptions of the FLRW model are spherical symmetry and isotropy of the universe. While this may be the state currently, there is no reason to believe that epochs of anisotropy did not exist in the early universe. Hence nonspherical spacetimes have become an active area of research in recent times.

A well-known result of the Jebsen-Birkhoff (1921, 1923) theorem is that spherically symmetric pulsating objects do not emit gravitational waves . Hence the recent detection of gravitational waves by LIGO, coordinated by Abbott *et al* (2016), has attracted increased interest in non-spherically symmetric solutions of Einstein's equations. In light of this, we give cognisance to plane symmetric spacetimes and hope to construct exact solutions that may be utilised to model perfect fluids. Such solutions may be of cosmological or astrophysical interest depending on the existence of a hypersurface of vanishing pressure. Note that spherical symmetry is a special case of plane symmetry.

Some early contributions to the study of plane symmetric perfect fluids include those conducted by Roy and Narain (1979) who generated plane symmetric models which represented fluid configurations for which the free gravitational fields were of Petrov type D. Tikekar (1980) demonstrated that plane symmetric conformally flat perfect fluid distributions are of class one, but that the converse is not true. That is, plane symmetric perfect fluid configurations of embedding class one are not necessarily conformally flat. Collins (1985) extended previous research involving static spherically symmetric spacetimes to include plane symmetry. He showed that, as in the case of spherical symmetry, a γ- law equation of state can be imposed on a plane symmetric perfect fluid, and he obtained the exact solution for general values of γ. Davis and Ray (1975) solved the Einstein–Dirac field equations for a ghost neutrino field and produced a model with shear, rotation and expansion. Sharif (2004) classified plane symmetric spacetimes according to matter collineations for both a degenerate and non-degenerate energy momentum tensor. Grøn and Soleng (1992) analysed static plane symmetric fields conformally related to a massless scalar field. Coley and Czapor (1992) examined the inheriting conformal Killing vector properties of plane symmetric perfect fluid spacetimes. Recently Zhang and Noh (2009) found an n-dimensional ($n \geq 4$) plane symmetric solution for which the source was a perfect fluid. Anguige (2000) proved the existence of a class of plane symmetric perfect fluid cosmologies that become Kasner-like on approach to the initial singularity. In more recent studies, Sharif and Siddiqa

(2010) investigated the final outcome of gravitational collapse resulting from the plane symmetric charged Vaidya spacetime, and provided a counter-example to the cosmic censorship conjecture. Also recently, LeFloch and Tchapnda (2011) considered plane symmetric spacetimes with positive cosmological constant where the matter was a stiff fluid. They found that the spacetime approaches the de Sitter spacetime while the matter disperses asymptotically.

The role of anisotropy within the field of cosmology has been demonstrated in various models of the universe ranging from inhomogeneous cosmologies, Lemaître-Tolman-Bondi cosmological models, dark energy inspired models, phantom cosmologies as well as braneworld models. Recently Maurya *et al* (2018) studied the role of pressure anisotropy in spherical models. Based on experimental observations, it is widely accepted that anisotropy played a fundamental role in the early expansion of the universe leading to structure formation, anisotropy in the CMBR, baryogenesis as well as the acceleration of the universe. These topics are well covered in the research works of Moroi and Murayana (2003), Fukushima (2016) as well as Saaidi and Hossienkhani (2011). While anisotropic solutions are simpler to obtain, the inclusion of pressure isotropy increases the mathematical complexity of the field equations, making them more difficult to solve. However there exists a large body of exact solutions for spherically symmetric spacetimes for isotropic perfect fluids. Delgaty and Lake (1998) listed all known solutions for spherically symmetric spacetimes. Unfortunately, such information is not as easily available in the case of plane symmetric distributions. The exterior of such systems are known to be described by the Kasner metric (1921) in the nonstatic case or the Taub metric(1951) for static spacetimes. In spherical symmetry, Birkhoff's theorem guarantees the existence of a unique exterior metric - the Schwarzschild solution, which is independent of whether the interior is static or nonstatic. There is no such analogue for plane symmetry.

The Kasner model presents a solution that is plane-symmetric as well as spatially homogenous, and is used in modeling the early-time evolution of the universe. The

Bianchi 1 model, which is obtained from the Kasner metric, has led to a large class of inhomogenous solutions, as well as large families of Bianchi models. Recently, Govender and Thirukkanesh (2014) studied relaxational effects in a Bianchi I cosmological model within the framework of extended irreversible thermodynamics. They showed that relaxational effects lead to a higher temperature of the cosmological fluid. The Belinsky-Khalatnikov-Lifshitz (BKL) (1982) model utilised the Kasner solution to describe the oscillatory nature of the universe around a gravitational singularity. The Mixmaster universe was a cosmological model proposed by Charles Misner (1969) in an attempt to understand the dynamics of the early universe. With just these few examples we note that the Kasner metric forms the background for the generation of a general family of cosmological solutions.

In this chapter we use the Kasner metric, together with a conformal transformation to generate and solve the Einstein field equations for a plane symmetric perfect fluid. As discussed in an earlier chapter, a conformal transformation is a mathematical technique that uses a known exact solution, referred to as a seed metric, to generate new solutions of Einstein's equations. By performing a conformal transformation of such a metric and involving a nonzero energy momentum tensor, solutions describing the gravitational field of a perfect fluid may be constructed. In this study we investigate whether a nonstatic solution with isotropic particle pressure can be established through the conformal transformations method on an anisotropic spacetime. We make use of the nonstatic, anisotropic Kasner metric as a seed solution and establish that this is indeed possible. Previous attempts by Hansraj (2012) to generate nonstatic models were unsuccessful. It was proved that spacetimes conformal to the Schwarzschild interior solution are necessarily static. Moreover, the plane symmetric Taub seed metric utilised by Hansraj (2013) did not yield nonstatic solutions.

This chapter is set out as follows : In §4.2 we present the Kasner metric, and use this metric as a seed to obtain the Einstein field equations for plane symmetric perfect fluids. We obtain an exact solution to the system of equations, and proceed to examine this solution for physical acceptability in §4.3. In § 4.4 a basic framework is outlined for future research on obtaining anisotropic solutions using the Kasner metric as a seed solution. We conclude with a discussion of our findings in §4.5 .

4.2 Vacuum Kasner Spacetime

The Kasner metric is often given in the form

$$ds^2 = -dt^2 + t^{2a}dx^2 + t^{2b}dy^2 + t^{2c}dz^2 \tag{4.2.1}$$

where a, b and c, known as the Kasner exponents, are real numbers satisfying

$$a + b + c = 1 = a^2 + b^2 + c^2 \tag{4.2.2}$$

Engelhardt *et al* (2015) showed that, in certain cases, one or more of the Kasner exponents are negative. When any of a, b or c is neither zero nor 1, there exists a curvature singularity at $t = 0$. In this case there is always at least one Kasner exponent that is negative. The metric (4.2.1) is a plane symmetric non-static solution of the vacuum Einstein field equations.

The Riemann tensor components for the spacetime (4.2.1) have the form

$$\frac{t^{2(1-a)}}{a(1-a)}R_{txtx} = \frac{t^{2(1-b)}}{b(1-b)}R_{tyty} = \frac{t^{2(1-c)}}{c(1-c)}R_{tztz} \quad = \quad 1$$

$$ct^{2c}R_{xyxy} = bt^{2b}R_{xzxz} = at^{2a}R_{yzyz} \quad = \quad abc$$

and it is clear that the Kasner metric is not flat as the Riemann tensor does not vanish in general. The Weyl tensor components are given by

$$t^{2(1-a)}C_{txtx} = -t^{2a}C_{yzyz} \quad = \quad a(1-a)$$

$$t^{2(1-b)}C_{tyty} = -t^{2b}C_{xzxz} \quad = \quad b(1-b)$$

$$-t^{2(1-c)}C_{tztz} = t^{2c}C_{xyxy} \quad = \quad c(1-c)$$

and we note that the Kasner metric is in general not conformally flat. A necessary condition for conformal flatness is $a = b = c$. However this violates condition (4.2.2). Hence we conclude that conformally flat Kasner metrics do not exist. The Kretschmann scalar has the following possible values

$$R^{abcd}R_{abcd} = \frac{4\left(3a^4 - 12a^3 + 20a^2 - 16a + 12\right)}{t^4} \qquad \text{or} \qquad \frac{4a^2\left(3a^2+4\right)}{t^4}$$

after invoking (4.2.2). This indicates that the metric has an irremovable curvature singularity at $t = 0$. We analyse the conformal counterpart to (4.2.1) which has the form

$$ds^2 = e^{2U(t,x)}\left(-dt^2 + t^{2a}dx^2 + t^{2b}dy^2 + t^{2c}dz^2\right) \tag{4.2.3}$$

where the conformal factor U is assumed to be a function of t and the space coordinate x. It can easily be shown that if the conformal factor is of the form $U(x)$ only, then the field equations force the homothety $U =$ constant. On the other hand if the form $U = U(t)$ is utilised then the relationships (4.2.2) will be violated. Our intention is to generate perfect fluid models using the seed geometry (4.2.1).

The Einstein tensor $\tilde{G}^a_b$ is given by

$$\tilde{G}^t_t = e^{-2U}\left[\frac{2}{t^{2a}}\left(U_{xx} + U_x^2\right) - 6U_t^2 - \frac{2}{t}U_t\right] \tag{4.2.4}$$

$$\tilde{G}^x_t = t^{-2a}\tilde{G}^t_x = 2e^{-2U}\left[U_{tx} - U_tU_x - \frac{a}{t}U_x\right] \tag{4.2.5}$$

$$\tilde{G}^x_x = e^{-2U}\left[-2\left(U_{tt} + U_t^2 + \frac{(b+c)}{t}U_t\right) - \frac{6}{t^{2a}}U_x^2\right] \tag{4.2.6}$$

$$\tilde{G}^y_y = e^{-2U}\left[\frac{2}{t^{2a}}\left(U_{xx} + U_x^2\right) - 2\left(U_{tt} + U_t^2 - \frac{(a+c)}{t}U_t\right)\right] \tag{4.2.7}$$

$$\tilde{G}^z_z = e^{-2U}\left[\frac{2}{t^{2a}}\left(U_{xx} + U_x^2\right) - 2\left(U_{tt} + U_t^2 - \frac{(a+b)}{t}U_t\right)\right] \tag{4.2.8}$$

Note we have repeatedly used (4.2.2) and elementary identities such as
$ac = \frac{1}{2}(a+c)^2 - \frac{1}{2}(a^2+c^2)$.

It is well known that the Kasner metric itself is anisotropic, however, we analyse whether this necessarily applies to its conformal counterpart. Requiring an isotropic particle pressure means that $\tilde{G}^x_x = \tilde{G}^y_y = \tilde{G}^z_z$. By comparing (4.2.7) and (4.2.8) we note that

$$\frac{a+c}{t}U_t = \frac{a+b}{t}U_t \tag{4.2.9}$$

since all the other terms in these two equations are the same. Solving (4.2.9) results in $\frac{U_t}{t}(b-c) = 0$, which leads to

$$b = c \qquad \text{or} \qquad U_t = 0 \tag{4.2.10}$$

First let us examine the consequences of $U_t = 0$. This means that the conformal factor has the form $U = U(x)$. However, this in turn implies that $U_x = 0$ by virtue of the vanishing of (4.2.5). That is, the conformal factor is constant thus giving a trivial homothetic transformation which is not interesting physically.

Next consider the implications of $b = c$. Using (4.2.2), this then implies that $b = c = 0$ and so $a = 1$ or $b = c = \frac{2}{3}$ which gives $a = -\frac{1}{3}$. We proceed to analyse each of these possibilities in turn.

4.2.1 The case $b = c = 0, a = 1$

The metric (4.2.3) assumes the simple form

$$ds^2 = e^{2U(t,x)}\left(-dt^2 + t^2dx^2 + dy^2 + dz^2\right) \tag{4.2.11}$$

and only one of the spatial directions is impacted by a function of time in the original metric.

The Einstein field equations are given by

$$\frac{2}{t^2}\left(U_{xx}+U_x^2\right)-6U_t^2-\frac{2}{t}U_t = -\mu e^{4U} \tag{4.2.12}$$

$$U_{tx}-U_tU_x-\frac{1}{t}U_x = 0 \tag{4.2.13}$$

$$-2\left(U_{tt}+U_t^2\right)+\frac{6}{t^2}U_x^2 = pe^{4U} \tag{4.2.14}$$

$$\frac{2}{t^2}\left(U_{xx}+U_x^2\right)-2\left(U_{tt}+U_t^2-\frac{1}{t}U_t\right) = pe^{4U} \tag{4.2.15}$$

To derive the general solution of (4.2.13) we begin by dividing (4.2.13) by U_x to obtain

$$\frac{U_{tx}}{U_x}=U_t+\frac{1}{t} \tag{4.2.16}$$

Integrating (4.2.16) with respect to t results in

$$\ln U_x = U+\ln t + c(x) \tag{4.2.17}$$

where $c(x)$ is a function of integration. Solving (4.2.17) yields

$$U_x = k(x)te^U \tag{4.2.18}$$

where $k(x)=e^{c(x)}$. We set

$$e^U=\phi(x,t) \tag{4.2.19}$$

and differentiate (4.2.19) with respect to x to obtain

$$e^UU_x=\phi' \tag{4.2.20}$$

so

$$U_x=\frac{\phi'}{e^U}=\frac{\phi'}{\phi} \tag{4.2.21}$$

Substituting (4.2.19) and (4.2.21) in (4.2.18) gives

$$\frac{\phi'}{\phi}=k(x)t\phi \tag{4.2.22}$$

which may be rewritten as

$$-\frac{\phi'}{\phi^2} = -k(x)t \tag{4.2.23}$$

Since $\left(\frac{1}{\phi}\right)_x = -\frac{\phi'}{\phi^2}$, we may express (4.2.23) as

$$\left(\frac{1}{\phi}\right)_x = -k(x)t \tag{4.2.24}$$

Integrating (4.2.24) with respect to x gives

$$\frac{1}{\phi} = -\left(t\int k(x)dx + g(t)\right) \tag{4.2.25}$$

from which we obtain the general solution to (4.2.13) as

$$e^U = -\left(th(x) + g(t)\right)^{-1} \tag{4.2.26}$$

where $h(x) = \int k(x)dx$ and $g(t)$ is a function of integration. This form immediately rules out the possibility of U being a separable function in general. Additionally, the isotropy condition (4.2.14) = (4.2.15) yields the constraint

$$U_{xx} - 2U_x^2 + tU_t = 0 \tag{4.2.27}$$

Substituting (4.2.26) into (4.2.27) we obtain the condition

$$g\left(h + \dot{g} + h''\right) + t\left[h^2 + h'^2 + h\left(\dot{g} + h''\right)\right] = 0 \tag{4.2.28}$$

where the dots and primes denote partial differentiation with respect to t and x respectively. Now equation (4.2.28) yields solutions only in certain special cases in view of the coupling of $g(t)$ and $h(x)$ and their derivatives. There are two cases that may lead to viable solutions.

- **Case 1**

  The presence of the factor t outside the second set of parenthesis motivates the form $g(t) = \alpha t$ for some constant α, which turns out to be inconsequential as it disappears. In this case equation (4.2.28) assumes the form

$$(\alpha + h)h'' + h'^2 + (h + \alpha)^2 = 0 \tag{4.2.29}$$

for the function $h(x)$. This equation is readily solvable in the form

$$h(x) = -\alpha \pm \sqrt{c_1 \cos \sqrt{2}x - c_2 \sin \sqrt{2}x} \tag{4.2.30}$$

where c_1 and c_2 are integration constants.

Taking the positive sign before the square root in (4.2.30) we obtain

$$U(t,x) = \ln \left[-\left(t\sqrt{c_1 \cos \sqrt{2}x - c_2 \sin \sqrt{2}x} \right)^{-1} \right]$$

for the conformal factor. In order to admit real-valued solutions, it is required that $t < 0$. The isotropic pressure and energy density are given by

$$p = \frac{t^2}{2}(7(c_2^2 - c_1^2)\cos 2\sqrt{2}x + 14c_1c_2 \sin 2\sqrt{2}x - (c_1^2 + c_2^2)) \tag{4.2.31}$$

$$\mu = \frac{t^2}{2}(5(c_2^2 - c_1^2)\cos 2\sqrt{2}x + 10c_1c_2 \sin 2\sqrt{2}x + (c_1^2 + c_2^2)) \tag{4.2.32}$$

for this case.

Under the conformal transformation $\bar{g}_{ab} = e^{2U} g_{ab}$, the transformed velocity field is given by

$$\bar{u}_a = \frac{1}{t\sqrt{c_1 \cos \sqrt{2}x - c_2 \sin \sqrt{2}x}},$$

and the following transformed kinematical quantities result:

$$\bar{\dot{u}}_a = \left(\frac{2}{t^2\sqrt{c_1\cos\sqrt{2}x - c_2\sin\sqrt{2}x}}, -\frac{c_2\cos\sqrt{2}x + c_1\sin\sqrt{2}x}{\sqrt{2}t\left(c_1\cos\sqrt{2}x - c_2\sin\sqrt{2}x\right)^{\frac{3}{2}}}\right.$$
$$\left., 0, 0\right) \tag{4.2.33}$$

$$\bar{\Theta} = 2\sqrt{c_1\cos\sqrt{2}x - c_2\sin\sqrt{2}x} \tag{4.2.34}$$

$$\bar{\omega}_{ab} = 0 \tag{4.2.35}$$

$$\bar{\sigma}_{ab} = \left(0, -\frac{2}{3\sqrt{c_1\cos\sqrt{2}x - c_2\sin\sqrt{2}x}},\right.$$
$$\left.\frac{1}{3t^2\sqrt{c_1\cos\sqrt{2}x - c_2\sin\sqrt{2}x}}, \frac{1}{3t^2\sqrt{c_1\cos\sqrt{2}x - c_2\sin\sqrt{2}x}}\right) \tag{4.2.36}$$

These calculations reveal that for this form of the conformal map, the fluid congruences are accelerating, expanding, shearing but irrotational in general.

Now considering the negative sign before the square root in (4.2.30), we obtain the conformal factor

$$U(t,x) = \ln\left[\frac{1}{t\sqrt{c_1\cos\sqrt{2}x - c_2\sin\sqrt{2}x)}}\right] \tag{4.2.37}$$

and the dynamical variables are given by

$$p = \frac{t^2}{2}\left(7(c_2^2 - c_1^2)\cos 2\sqrt{2}x + 14c_1c_2\sin 2\sqrt{2}x - (c_1^2 + c_2^2)\right) \tag{4.2.38}$$

$$\mu = \frac{t^2}{2}\left(5(c_2^2 - c_1^2)\cos 2\sqrt{2}x + 10c_1c_2\sin 2\sqrt{2}x + (c_1^2 + c_2^2)\right) \tag{4.2.39}$$

and the transformed kinematical quantities are as follows :

$$\bar{\dot{u}}_a = \left(-\frac{2}{t^2\sqrt{c_1\cos\sqrt{2}x - c_2\sin\sqrt{2}x}},\right.$$
$$\left.\frac{c_2\cos\sqrt{2}x + c_1\sin\sqrt{2}x}{\sqrt{2}t\left(c_1\cos\sqrt{2}x - c_2\sin\sqrt{2}x\right)^{\frac{3}{2}}}, 0, 0\right) \tag{4.2.40}$$

$$\bar{\Theta} = -2\sqrt{c_1\cos\sqrt{2}x - c_2\sin\sqrt{2}x} \tag{4.2.41}$$

$$\bar{\omega}_{ab} = 0 \tag{4.2.42}$$

$$\bar{\sigma}_{ab} = \left(0, \frac{2}{3\sqrt{c_1\cos\sqrt{2}x - c_2\sin\sqrt{2}x}}, -\frac{1}{3t^2\sqrt{c_1\cos\sqrt{2}x - c_2\sin\sqrt{2}x}},\right.$$
$$\left.-\frac{1}{3t^2\sqrt{c_1\cos\sqrt{2}x - c_2\sin\sqrt{2}x}}\right) \tag{4.2.43}$$

In this case, the perfect fluid is accelerating, collapsing, shearing and non-rotating. Note also that this solution corresponds to $t > 0$.

The metric (4.2.11) may now be written explicitly as

$$ds^2 = \left[\frac{1}{t^2(c_1\cos\sqrt{2}x - c_2\sin\sqrt{2}x)}\right](-dt^2 + t^2dx^2 + dy^2 + dz^2)$$

- **Case 2**

Equation (4.2.28) may also be solved with the form $h(x) = K$, where K is a constant. In this case we obtain

$$(\dot{g} + K)(g + Kt) = 0 \tag{4.2.44}$$

which is satisfied by $g(t) = -Kt + L$ for some new constant L or just $g(t) = -Kt$ for the second bracket. Substituting this back into the conformal factor reveals that the conformal factor U must be a constant, thus yielding a homothety which does not lead to any new physics.

4.2.2 The case $b = c = \frac{2}{3}$, $a = -\frac{1}{3}$

For this combination of exponents, the line element (4.2.3) assumes the form

$$ds^2 = e^{2U(t,x)} \left(-dt^2 + t^{-\frac{2}{3}} dx^2 + t^{\frac{4}{3}} dy^2 + t^{\frac{4}{3}} dz^2 \right) \tag{4.2.45}$$

The Einstein field equations are written as

$$2t^{\frac{2}{3}} \left(U_{xx} + U_x^2 \right) - 6U_t^2 - \frac{2}{t} U_t = -\mu e^{4U} \tag{4.2.46}$$

$$U_{tx} - U_t U_x + \frac{1}{3t} U_x = 0 \tag{4.2.47}$$

$$-2 \left(U_{tt} + U_t^2 + \frac{4}{3t} U_t \right) - 6t^{\frac{2}{3}} U_x^2 = pe^{4U} \tag{4.2.48}$$

$$2t^{\frac{2}{3}} \left(U_{xx} + U_x^2 \right) - 2 \left(U_{tt} + U_t^2 - \frac{4}{3t} U_t \right) = pe^{4U} \tag{4.2.49}$$

Using the method outlined for the solution of (4.2.13) we solve the equation (4.2.47) and obtain the functional form

$$e^U = \left(g(t) - t^{-\frac{1}{3}} \int k(x) dx \right)^{-1} \tag{4.2.50}$$

which takes the simpler form

$$e^U = \left(g(t) - t^{-\frac{1}{3}} h(x) \right)^{-1} \tag{4.2.51}$$

where we have put $h(x) = \int k(x)dx$.

Then equating (4.2.48) and (4.2.49) to get the isotropy condition yields the equation

$$U_{xx} + 4U_x^2 + \frac{8}{3} t^{-\frac{5}{3}} U_t = 0 \tag{4.2.52}$$

which must be solved in conjunction with equation (4.2.51). Inserting (4.2.51) into (4.2.52) yields the equation

$$9t^{\frac{8}{3}} \left[h'' \left(h - gt^{\frac{1}{3}} \right) + 3h'^2 \right] - \left(8h + 24t^{\frac{4}{3}} \dot{g} \right) \left(h - gt^{\frac{1}{3}} \right) = 0 \tag{4.2.53}$$

Again, the functions $h(x)$ and $g(t)$ are inseparable so special cases could be attempted. Setting $h(x) = q$, a constant, yields $g(t) = qt^{-1/3} + s$ where s is an integration constant. This form results in a constant conformal factor and so is not examined any further. There remains the option $g(t) = c_3$, where c_3 is a constant. However, the consequence of this choice is that (4.2.53) assumes the form

$$9t^{\frac{8}{3}}\left[h''\left(h - c_3 t^{\frac{1}{3}}\right) + 3h'^2\right] - 8h\left(h - c_3 t^{\frac{1}{3}}\right) = 0 \tag{4.2.54}$$

which is a second order nonlinear differential equation in $h(x)$. This equation is not readily solvable. There does not appear to exist any further solutions to (4.2.53).

4.2.3 Physical Properties of the Model

The speed of sound in a nonstatic perfect fluid was discussed by Knutsen (1984) as well as Cahill and Taub (1971) and was shown to be given by $v^2 = \frac{dp/dt}{d\mu/dt}$ for an adiabatic system with a constant entropy. This followed from the deduction of Nariai (1967) that adiabatic flows are characterised by entropy functions that are time independent. Accordingly, from our results in section 4.2.1, we obtain

$$\frac{dp}{d\mu} = -\frac{c_1^2 + c_2^2 + 7(c_1^2 - c_2^2)\cos 2\sqrt{2}x - 14c_1c_2 \sin 2\sqrt{2}x}{c_1^2 + c_2^2 + 5(c_2^2 - c_1^2)\cos 2\sqrt{2}x + 10c_1c_2 \sin 2\sqrt{2}x} \tag{4.2.55}$$

as the sound speed index. It is demanded that $0 < \frac{dp}{d\mu} < 1$ to ensure a subluminal sound speed.

An examination of the associated plots reveals that the model constructed displays pleasing physical behaviour. Figure 4.1 and Figure 4.2 reflect a density and pressure profile that is smooth and singularity-free. Figure 4.3 depicts the sound speed index $\frac{dp}{d\mu}$ and it may be noted that the requirement $0 < \frac{dp}{d\mu} < 1$ is satisfied everywhere. This ensures that the speed of sound never exceeds the speed of light in this fluid. In the central region, where $x = 0$, we get $\frac{dp}{d\mu} = \frac{4c_1^2 - 3c_2^2}{2c_1^2 - 3c_2^2} = \frac{4\beta - 3}{2\beta - 3}$, where we have put $\beta = \frac{c_1^2}{c_2^2}$. For $\frac{dp}{d\mu} > 0$ we get $0 < \beta < \frac{3}{4}$ or $\beta > \frac{3}{2}$. For $\frac{dp}{d\mu} < 1$ we obtain $0 < \beta < \frac{3}{2}$. This suggests that acceptable values for the integration constants c_1 and c_2 must satisfy $0 < \frac{dp}{d\mu} = \frac{c_1^2}{c_2^2} < \frac{3}{4}$

for a causal speed of sound. It is interesting to observe that the matter variables are well-behaved even though we did not specify an equation of state between the energy density and pressure.

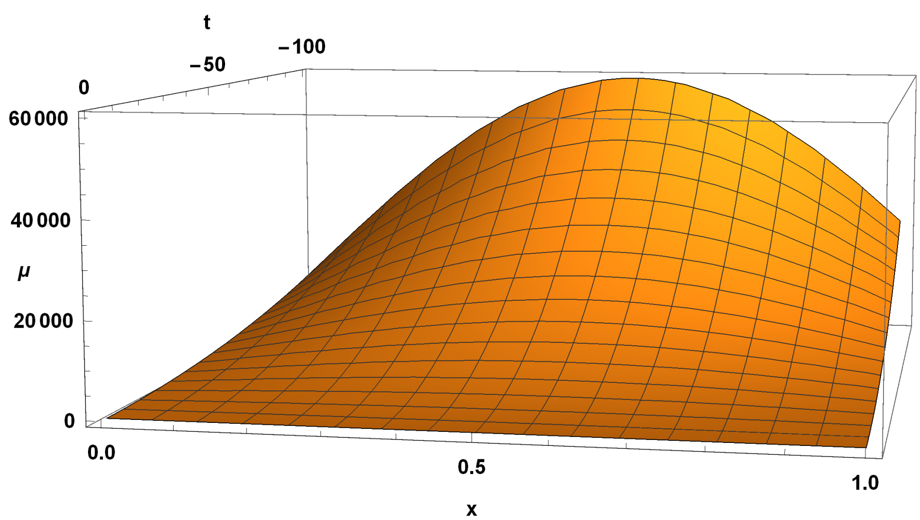

Figure 4.1: Energy density μ as a function of t and x

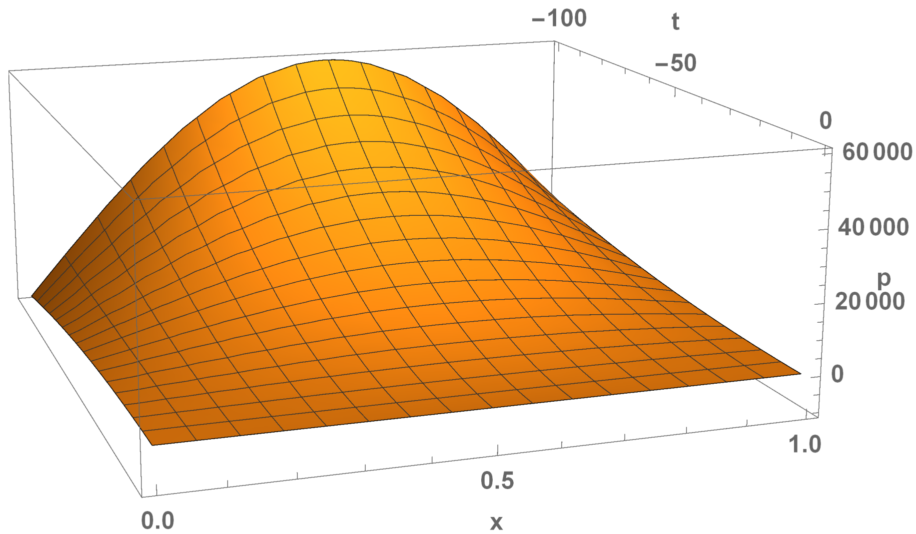

Figure 4.2: Pressure p as a function of t and x

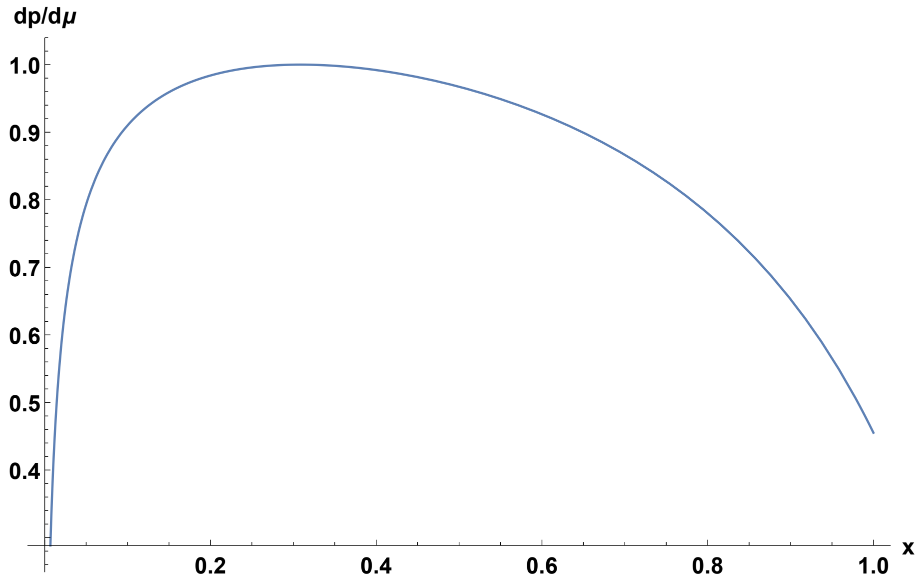

Figure 4.3: Sound-speed $\frac{dp}{d\mu}$ as a function of x

4.3 Anisotropic Solutions

The condition of pressure isotropy proved to be restrictive in solving the field equations. If the condition of pressure isotropy is relaxed, then new classes of anisotropic models may be found. This is part of future research for which a preliminary framework has been mapped out. The solution to (4.2.5), $U_{tx} - U_t U_x - \frac{a}{t} U_x = 0$, is $e^U = -\left(t^a h(x) + g(t)\right)^{-1}$, from which we obtain $U(t,x) = -\ln(-g(t) - t^a h(x))$. The Kasner metric represents a spacetime with three spatial directions x, y and z. We can consider isotropy in any two directions at a time. We investigate the following possibilities:

- $\tilde{G}^x_x = \tilde{G}^y_y$, which yields the equation

$$U_{xx} + 4U_x^2 = -t^{2a-1}(1+c)U_t \tag{4.3.1}$$

Equation (4.3.1) must be solved in conjunction with (4.2.5). Following similar procedure as discussed previously, the general solution of $\tilde{G}^x_t = 0$ is $e^U = -(t^a h(x) + g(t))^{-1}$. Putting $\Delta = t^a h(x) + g(t)$, we have

$$\begin{aligned} \Delta_x &= t^a h' \\ \Delta_t &= a t^{a-1} h + \dot{g} \end{aligned}$$

Rewriting $e^U = -\Delta^{-1}$, we obtain

$$U_x = \frac{t^a h'}{-\Delta} \tag{4.3.2}$$

$$U_{xx} = \frac{-\Delta t^a h'' - t^{2a} h'^2}{\Delta^2} \tag{4.3.3}$$

$$U_t = \frac{a t^{a-1} h + \dot{g}}{-\Delta} \tag{4.3.4}$$

Feeding (4.3.2) - (4.3.4) into (4.3.1) gives

$$-(t^a h + g)t^{2a} h'' + 3t^{2a} h'^2 = t^{2a-1}(1+c)(a t^{a-1} h + \dot{g})(t^a h + g) \tag{4.3.5}$$

As mentioned previously, it may easily be demonstrated with elementary algebra that the Kasner conditions $a + b + c = 1$ and $a^2 + b^2 + c^2 = 1$ imply that at least one of a, b or c is negative except in the case where any two are zero. In this case the spacetime is still nontrivial as one spatial direction is impacted by a time-dependent function. A comprehensive analysis that will allow for a solution of (4.3.5) requires of us to find suitable values of a, b and c. This is a formidable task which falls outside the scope of this dissertation.

- $\tilde{G}^x_x = \tilde{G}^z_z$, for which we obtain

$$U_{xx} + 4U_x^2 = -t^{2a-1}(1+b)U_t \tag{4.3.6}$$

Solving (4.3.6) in conjunction with (4.2.5) yields

$$-(t^a h + g)t^{2a}h'' + 3t^{2a}h'^2 = t^{2a-1}(1+b)(at^{a-1}h + \dot{g})(t^a h + g) \tag{4.3.7}$$

which is equivalent to the previous case with $b = c$. Therefore we do not repeat the discussion.

- $\tilde{G}^y_y = \tilde{G}^z_z$, which results in the condition

$$U_t = 0 \tag{4.3.8}$$

This implies that $U = U(x)$. However, it has been shown earlier that this is not a worthwhile case. Alternatively we must have $b = c$ and in turn we obtain $a = -\frac{1}{3}$, $b = c = \frac{2}{3}$ or $a = 1$, $b = c = 0$.

- Finally all isotropy cases may be relaxed and we may arbitrarily choose functions for $h(x)$ and $g(t)$ which satisfy (4.2.5).

With maximal anisotropy and a linear barotropic equation of state in the x-direction, given by $p_x = \alpha\mu$, which is tantamount to

- $\tilde{G}^x_x = \alpha\tilde{G}^t_t$. The equation

$$(1-\alpha)(U_{xx} + U_x^2) = t^{2a}U_{tt} + (1+3\alpha)t^{2a}U_t^2 - (a+b+\alpha)t^{2a-1}U_t \tag{4.3.9}$$

arises, which must be solved in conjunction with $e^U = -(t^a h(x) + g(t))^{-1}$. This will be the subject of future research.

We are optimistic this approach will lead to new classes of anisotropic solutions.

4.4 Discussion

In this investigation, we commenced with the Kasner metric as a seed solution. The conformal mappings method was applied to this metric which was known to be plane symmetric, nonstatic and anisotropic. Two classes of solutions that modeled isotropic spacetimes were generated up to branch cuts. Both sets of solutions represented fluid congruences that were accelerating, shearing and nonrotating. However, one model was expanding while the other was in collapse. An interesting phenomenon predicted by this model is the possibility of observing blueshifts as the model oscillates between two stable states. The models generated possessed pleasing physical properties which are consistent with a cosmological fluid. At the basic level, the surfaces of density and pressure were smooth, well-behaved and singularity free. The speed of sound was found to be less than the speed of light, thus affirming causality and stability. We have thus succeeded in constructing a viable cosmological fluid distribution with pressure isotropy. The exact solution may be useful in the study of gravitational waves. We also briefly analysed the consequence of relaxing the conditions of pressure isotropy. The resulting equations were no less intricate than for the isotropic cases. In order to not stray beyond the ambit of this dissertation, we have consigned a thorough investigation of these cases to a future study.

Chapter 5

Spherically Symmetric Radiating Fluids

5.1 Introduction

Spherically symmetric spacetimes play a hugely important role in the study of general relativity. They are reasonably simple, yet crucial to our understanding of the many astrophysical objects which have been found to be very nearly spherical, as noted by Schutz (2009). Cosmological models, including the Friedmann-Robertson-Walker solutions, inhomogenous models as well as dark energy inspired models employ spherical symmetry. This is largely due to Copernican Principle. This chapter, which focuses on the collapse of a radiating star, takes us on a journey of spherically symmetric systems and concludes with an examination of the role played by an equation of state on the dynamical (in)stability of a star undergoing dissipative collapse.

The phenomenon of gravitational collapse has become a widely investigated subject due to its many interesting applications in astrophysics. The first attempt at modeling the collapse of a spherically symmetric matter distribution in the form of a dust cloud and having a Schwarzschild exterior was carried out by Oppenheimer and Snyder (1939). Taking into consideration that a radiating collapsing mass distribution has outgoing energy, its exterior spacetime is no longer a vacuum but contains null radiation. In this regard, Vaidya (1951) obtained an exact solution to the Einstein field equations which describe the exterior field of a radiating spherically symmetric fluid. Santos (1985) derived the junction conditions for a spherically symmetric star undergoing shear-free dissipative collapse in the form of a radial heat flux. This pioneering work allowed for the matching of the interior and exterior spacetimes of a collapsing star, and paved the way for the study of dissipative gravitational collapse. Interesting developments on the subject of dissipative collapse have since been made by authors such as Misner and Sharp (1964), de Oliveira and Santos (1987), Tomimura and Nunes (1993), Chan (2000), Maharaj and Govender (2000), Govender *et al* (2003) and Herrera *et al* (2008).

When a system in an initial state of static equilibrium experiences a disturbance or a perturbation, the stability of that system is affected. Dynamical stability is the property of a system to retain its stable state under small perturbations. The stability problem is an important one in the study of self-gravitating objects because a stellar model which proves to be stable under collapse is potentially a physically realistic model. Also, depending on the extent of instability of a system in collapse, the resulting patterns of evolution will vary. Hence the stability problem has become a subject of much investigation.

Chandrasekhar (1964) was the first to examine the dynamical instability of a spherically symmetric mass with isotropic pressure. With the aid of the adiabatic index Γ, he showed that for a system to remain stable under collapse, Γ must exceed $\frac{4}{3}$. Following this, much has been written in the literature about dynamical instability. Herrera et al (1989) studied the instability range for a non-adiabatic sphere and showed that relativistic corrections as a result of heat flow decreases the unstable range of Γ and renders the fluid less unstable. Chan et al (1993) investigated the stability criteria by deviating from the perfect fluid condition in two ways: they considered the effect of radiation in the free-streaming approximation, and they assumed the presence of local anisotropy of the fluid. Herrera et al (2012) also examined the dynamical instability of expansion-free, locally anisotropic spherical stellar bodies. The stability problem for collapsing matter configurations has been extended to include the effect of charge, higher dimensions and higher order effects such as Gauss-Bonnet's contribution to the internal core.

In this work, we consider a spherically symmetric static configuration undergoing radiative collapse. We assume shear-free and isotropic conditions. A linear equation of state of the form $p_r = \gamma\mu$ is imposed on the perturbed radial pressure and energy density, and the complete gravitational behaviour of the collapsing star is obtained. The stability ranges have been explored through the adiabatic index Γ for the Newtonian and post-Newtonian regimes.

The structure of this chapter is as follows: In §5.2 we introduce the field equations describing the geometry and matter content for a star undergoing shear-free gravitational collapse. In §5.3 the exterior spacetime is presented by way of the Vaidya metric. The focus of §5.4 are the junction conditions necessary for the smooth matching of the interior spacetime with Vaidya's exterior solution across the boundary. In §5.5 the perturbative scheme is described and the field equations for the static and perturbed configurations are given. In this section we also present the temporal equation employed by the perturbative scheme that begins with an initially static star that is perturbed so that the perturbations decay exponentially with time. §5.6 presents a static and a radiating model. We discuss dissipative collapse, express the perturbed quantities in terms of two unspecified variables and introduce an equation of state which allows us to express the perturbed quantities in terms of r only. We explore the stability of our collapsing model in the Newtonian and post-Newtonian approximations in §5.7, and our results are discussed in §5.8.

5.2 Interior Spacetime

The line element for the interior of a spherically symmetric, shear-free spacetime in simultaneously comoving and isotropic coordinates is

$$ds^2 = -A^2 dt^2 + B^2[dr^2 + r^2(d\theta^2 + \sin^2\theta d\phi^2)] \tag{5.2.1}$$

where $A = A(t,r)$ and $B = B(t,r)$ are the metric functions.
The energy-momentum tensor for the interior matter distribution is given by

$$T_{ab} = (\mu + p_t)w_a w_b + p_t g_{ab} + (p_r - p_t)X_a X_b + q_a w_b + q_b w_a, \tag{5.2.2}$$

where μ is the energy density, p_r the radial pressure, p_t the tangential pressure and q_a the heat flux. The four-velocity of the fluid is denoted by w_a and X_a is a unit four-vector along the radial direction. These quantities must satisfy the conditions

$$\begin{aligned} w_a w^a &= -1 \\ w_a q^a &= 0 \\ X_a X^a &= 1 \\ X_a w^a &= 0 \end{aligned}$$

Furthermore, in comoving coordinates we have

$$\begin{aligned} w^a &= A^{-1}\delta^a_0 \\ q^a &= q\delta^a_1 \\ X^a &= B^{-1}\delta^a_1 \end{aligned}$$

The nonzero components of the Einstein field equations for the line element (5.2.1) and the energy momentum (5.2.2) are

$$\mu = -\frac{1}{B^2}\left[2\frac{B''}{B} - \left(\frac{B'}{B}\right)^2 + \frac{4}{r}\frac{B'}{B}\right] + \frac{3}{A^2}\left(\frac{\dot{B}}{B}\right)^2, \tag{5.2.3}$$

$$\begin{aligned} p_r &= \frac{1}{B^2}\left[\left(\frac{B'}{B}\right)^2 + \frac{2}{r}\left(\frac{A'}{A} + \frac{B'}{B}\right) + 2\frac{A'}{A}\frac{B'}{B}\right] \\ &\quad + \frac{1}{A^2}\left[-2\frac{\ddot{B}}{B} - \left(\frac{\dot{B}}{B}\right)^2 + 2\frac{\dot{A}}{A}\frac{\dot{B}}{B}\right] \end{aligned} \tag{5.2.4}$$

$$\begin{aligned} p_t &= \frac{1}{A^2}\left[-2\frac{\ddot{B}}{B} - \left(\frac{\dot{B}}{B}\right)^2 + 2\frac{\dot{A}}{A}\frac{\dot{B}}{B}\right] \\ &\quad + \frac{1}{B^2}\left[\frac{B''}{B} - \left(\frac{B'}{B}\right)^2 + \frac{1}{r}\left(\frac{A'}{A} + \frac{B'}{B}\right) + \frac{A''}{A}\right] \end{aligned} \tag{5.2.5}$$

$$q = \frac{2}{AB^2}\left[\frac{\dot{B}'}{B} - \frac{\dot{B}}{B}\left(\frac{B'}{B} + \frac{A'}{A}\right)\right] \tag{5.2.6}$$

where dots and primes represent partial derivatives with respect to t and r respectively. This is a system of coupled partial differential equations in the variables A, B, μ, p and q.

The anisotropic parameter, Δ, is defined as the difference between the radial and tangential pressures in a stellar fluid distribution. In other words,

$$\Delta = p_t - p_r. \tag{5.2.7}$$

Pressure isotropy means that the radial pressure is equal to the tangential pressure, implying that $\Delta = 0$ in equation (5.2.7). By employing the condition for pressure isotropy, we are able to eliminate p_r and p_t from equations (5.2.4) and (5.2.5). The field equations (5.2.4) and (5.2.5) may then be written more concisely as

$$\frac{A''}{A} + \frac{B''}{B} = \left(2\frac{B'}{B} + \frac{1}{r}\right)\left(\frac{A'}{A} + \frac{B'}{B}\right). \tag{5.2.8}$$

A solution of equation (5.2.8) enables us to describe the interior matter distribution and the physical behaviour of the system. It is interesting to observe that if we redefine the radial coordinate r by

$$x = r^2$$

then we generate the differential equation

$$(AB^{-1})_{xx} = 2A(B^{-1})_{xx}$$

which is a more compact form of (5.2.8).

5.3 Exterior Spacetime and the Vaidya Solution

Spacetime is divided by the boundary of a star into two distinct regions, the interior and exterior regions, represented by $\mathcal{M}^-$ and $\mathcal{M}^+$ respectively. The interior region is described by the metric (5.2.1). The exterior gravitational field of the radiating star is given by the Vaidya (1951)solution, for which the line element is

$$ds_+^2 = -\left[1 - \frac{2m(v)}{r}\right] dv^2 - 2dvdr + r^2 d\theta^2 + r^2 \sin^2\theta d\phi^2 \qquad (5.3.1)$$

where $m(v)$ represents the Newtonian mass of the gravitating body as measured by an observer at infinity. The solution (5.3.1) is the unique spherically symmetric solution of the Einstein field equations for radiation in the form of a null fluid. The Vaidya solution is often used in applications in astrophysics. In their respective investigations on the collapse of radiating stars, de Oliveira *et al* (1985), Kolassis *et al* (1988) and Kramer (1992) are just a few of the many authors who have used the Vaidya solution to describe the exterior gravitational field of the star. The Vaidya solution (5.3.1) is completely determined by the mass function $m(v)$. In order for the exterior spacetime of the radiating star to be physically realistic, it is a requirement that $\frac{dm}{dv} \leq 0$. In other words , $m(v)$ must be a decreasing function. This requirement is motivated by the fact that the mass of the collapsing star must decrease as a result of a loss of energy in the form of radiation.

5.4 Junction Conditions

We consider a spherical surface described by a timelike three-space Σ which divides the spacetime into two distinct regions $\mathcal{M}^-$ and $\mathcal{M}^+$. In this section the junction conditions are generated for the Einstein field equations with cosmological constant $\Lambda = 0$. The junction conditions are then used to match the interior and exterior regions of the spherically symmetric spacetime.

Let g_{ij} be the intrinsic metric to Σ so that

$$ds^2_\Sigma = g_{ij} d\phi^i d\phi^j \tag{5.4.1}$$

The intrinsic coordinates to Σ are given by ϕ^i where $i = 1, 2, 3$. The line elements in the regions $\mathcal{M}^\pm$ are of the form

$$ds^2{}_\pm = g_{ab} d\mathcal{X}^a_\pm d\mathcal{X}^b_\pm \tag{5.4.2}$$

The coordinates in $\mathcal{M}^\pm$ are $\mathcal{X}^a_\pm$ where $a = 0, 1, 2, 3$. We require that the metrics (5.4.1) and (5.4.2) match smoothly across Σ. This generates the first junction condition

$$(ds^2_-)_\Sigma = (ds^2_+)_\Sigma = ds^2_\Sigma \tag{5.4.3}$$

The notation $(\ )_\Sigma$ denotes the value of $(\ )$ on Σ. Consequently the coordinates of Σ in $\mathcal{M}^\pm$ are given by $\mathcal{X}^a_\pm = \mathcal{X}^a_\pm(\xi^i)$. The second junction condition is obtained by requiring continuity of the extrinsic curvature of Σ across the boundary. This gives

$$K^+_{ij} = K^-_{ij} \tag{5.4.4}$$

where

$$K^\pm_{ij} \equiv -n^\pm_a \frac{\partial^2 \mathcal{X}^a_\pm}{\partial\phi^i \partial\phi^j} - n^\pm_a \Gamma^a{}_{cd} \frac{\partial \mathcal{X}^c_\pm}{\partial\phi^i} \frac{\partial \mathcal{X}^d_\pm}{\partial\phi^j} \tag{5.4.5}$$

and $n^\pm_a(\mathcal{X}^b_\pm)$ are the components of the vector normal to Σ. Listed below are the spacetime conditions necessary for the second junction condition (5.4.4) to be valid

$$m(v) = \left(\frac{r^3 B}{2A^2} \dot{B}^2 - r^2 B' - \frac{r^3}{2B} B'^2 \right)_\Sigma \tag{5.4.6}$$

$$p_\Sigma = (qB)_\Sigma \tag{5.4.7}$$

Thus the two junction conditions to be satisfied across the boundary are

$$\left(K_{ij}^{+} - K_{ij}^{-}\right)_{\Sigma} = 0 \tag{5.4.8}$$

and

$$\left(ds_{+}^{2} - ds_{-}^{2}\right)_{\Sigma} = 0 \tag{5.4.9}$$

A comprehensive review of junction conditions for boundary surfaces with applications to general relativity is provided by Lake (1987).

5.5 The Perturbed Equations

We assume that the fluid is initially in static equilibrium, hence the fluid is described by quantities that are not time-dependent, ie they are expressed in terms of the radial-coordinate only. It is then asserted that the static system is perturbed, undergoing slow shear-free collapse and producing pure radiation. The quantities such as energy density, radial pressure and tangential pressure of the static system are denoted by a zero subscript and those of the perturbed fluid by an overhead bar. We further assume that the metric functions $A(r,t)$ and $B(r,t)$ have the same time dependence in their perturbations. This assumption would imply that the perturbed material functions also have the same time dependence. Therefore the metric functions and the material functions are given by

$$\begin{aligned} A(r,t) &= A_0(r) + \epsilon a(r)T(t) && (5.5.1)\\ B(r,t) &= B_0(r) + \epsilon b(r)T(t) && (5.5.2)\\ \mu(r,t) &= \mu_0(r) + \epsilon\bar{\mu}(r,t) && (5.5.3)\\ p_r(r,t) &= p_{r0}(r) + \epsilon\bar{p}_r(r,t) && (5.5.4)\\ p_t(r,t) &= p_{t0}(r) + \epsilon\bar{p}_t(r,t) && (5.5.5)\\ m(r,t) &= m_0(r) + \epsilon\bar{m}(r,t) && (5.5.6) \end{aligned}$$

where we assume that $0 < \epsilon \ll 1$

Einstein's field equations for the static configuration are

$$\mu_0 = -\frac{1}{B_0^2}\left[2\frac{B_0''}{B_0} - \left(\frac{B_0)'}{B_0}\right)^2 + \frac{4}{r}\frac{B_0'}{B_0}\right] \tag{5.5.7}$$

$$p_{r0} = \frac{1}{B_0^2}\left[\left(\frac{B_0'}{B_0}\right)^2 + \frac{2}{r}\left(\frac{A_0'}{A_0} + \frac{B_0'}{B_0}\right) + 2\frac{A_0'}{A_0}\frac{B_0'}{B_0}\right] \tag{5.5.8}$$

$$p_{t0} = \frac{1}{B_0^2}\left[\frac{B_0''}{B_0} - \left(\frac{B_0'}{B_0}\right)^2 + \frac{1}{r}\left(\frac{A_0'}{A_0} + \frac{B_0'}{B_0}\right) + \frac{A_0''}{A_0}\right] \tag{5.5.9}$$

The perturbed field equations up to first order in ϵ can be written as

$$\begin{aligned}\bar{\mu} = {} & -3\mu_0\frac{b}{B_0}T \\ & +\frac{1}{B_0^3}\left[-\left(\frac{B_0'}{B_0}\right)^2 b + 2\left(\frac{B_0'}{B_0} - \frac{2}{r}\right)b' - 2b''\right]T\end{aligned} \tag{5.5.10}$$

$$\begin{aligned}\bar{p}_r = {} & -2p_{r0}\frac{b}{B_0}T \\ & +\frac{2}{B_0^2}\left[\left(\frac{B_0'}{B_0} + \frac{1}{r} + \frac{A_0'}{A_0}\right)\left(\frac{b}{B_0}\right)' + \left(\frac{B_0'}{B_0} + \frac{1}{r}\right)\left(\frac{a}{A_0}\right)'\right]T \\ & -2\frac{b}{A_0^2 B_0}\ddot{T}\end{aligned} \tag{5.5.11}$$

$$\begin{aligned}\bar{p}_t = {} & -2p_{t0}\frac{b}{B_0}T \\ & +\frac{1}{B_0^2}\left[\left(\frac{b}{B_0}\right)'' + \frac{1}{r}\left(\frac{b}{B_0}\right)' + 2\frac{A_0'}{A_0}\left(\frac{a}{A_0}\right)' + \left(\frac{a}{A_0}\right)'' + \frac{1}{r}\left(\frac{a}{A_0}\right)'\right]T \\ & -2\frac{b}{A_0^2 B_0}\ddot{T}\end{aligned} \tag{5.5.12}$$

$$qB = \frac{2}{B_0}\left(\frac{b}{A_0 B_0}\right)'\dot{T} \tag{5.5.13}$$

The total energy entrapped up to radius r inside Σ for the static and perturbed configurations are respectively given by

$$m_0(r_\Sigma) = -\left(r^2 B_0' + \frac{r^3 {B_0'}^2}{2B_0}\right)_\Sigma \tag{5.5.14}$$

$$\bar{m}(r_\Sigma, t) = -\left(\left[r^2 b' + \frac{r^3 {B_0'}^2}{2B_0}\left(2\frac{b'}{B_0'} - \frac{b}{B_0}\right)\right] T(t)\right)_\Sigma \tag{5.5.15}$$

The smooth matching of the interior spacetime to the Vaidya exterior is facilitated by using the junction conditions derived by Santos (1985), and we may rewrite equations (5.5.11) and (5.5.13) as

$$\bar{p}_r = -2p_{r0}\frac{b}{B_0}T + \frac{2b}{A_0^2 B_0}\left(\alpha T - \ddot{T}\right) \tag{5.5.16}$$

and

$$qB = \frac{4b}{A_0^2 B_0}\beta\dot{T} \tag{5.5.17}$$

where

$$\alpha(r) = \frac{A_0^2}{B_0 b}\left[\left(\frac{B_0'}{B_0} + \frac{1}{r} + \frac{A_0'}{A_0}\right)\left(\frac{b}{B_0}\right)' + \left(\frac{B_0'}{B_0} + \frac{1}{r}\right)\left(\frac{a}{A_0}\right)'\right] \tag{5.5.18}$$

$$\beta(r) = \frac{A_0^2}{2b}\left(\frac{b}{A_0 B_0}\right)' \tag{5.5.19}$$

We make use of the junction condition $(\bar{p}_r)_\Sigma = (qB)_\Sigma$ together with the fact that $(p_{r0})_\Sigma = 0$ to obtain

$$\alpha_\Sigma T - \ddot{T} = 2\beta_\Sigma \dot{T} \tag{5.5.20}$$

which has a particular solution given by

$$T(t) = -\exp\left[\left(-\beta_\Sigma + \sqrt{\alpha_\Sigma + \beta_\Sigma^2}\right)t\right] \tag{5.5.21}$$

where we have assumed that $\alpha_\Sigma > 0$ and $\beta_\Sigma < 0$. This solution represents a system in static equilibrium that starts to collapse at $t = -\infty$ and continues to collapse as t increases. The solution (5.5.21) has been used by many authors investigating gravitational collapse. The solution formed the basis of the work of Chan *et al* (1993) in which they investigated the dynamical instability for radiating anisotropic collapse. In more recent times, Govender *et al* (2014) used the solution in their investigation on the role of shear in dissipative collapse.

5.6 A Radiating Model

In order to provide an analysis of the collapse process, we select a particular model in which the following quantities are specified as follows:

$$A_0(r) = c_1 - \frac{c_2\left(1-r^2\right)}{1+r^2} \tag{5.6.1}$$

$$B_0(r) = \frac{2R}{1+r^2} \tag{5.6.2}$$

$$T(t) = -e^{\lambda t} \tag{5.6.3}$$

where c_1 , c_2 and R are constants and $\lambda = -\beta_\Sigma + \sqrt{\alpha_\Sigma + \beta_\Sigma^2}$. Then (5.5.7) and (5.5.8) can be written as

$$\mu_0 = \frac{3}{R^2} \tag{5.6.4}$$

$$p_{r0} = -\frac{c_1 - 3c_2 + r^2\left(c_1 + 3c_2\right)}{R^2\left(c_1 - c_2 + r^2\left(c_1 + c_2\right)\right)} \tag{5.6.5}$$

Using (5.5.1) - (5.5.6) together with (5.6.1) - (5.6.3) we obtain the perturbative quantities as follows :

$$\begin{aligned}\bar{\mu} &= \frac{e^{\lambda t}\left(r^2+1\right)}{4rR^3}\Big[2r\left(r^2+9\right)b(r)\\ &\quad+\left(4r^4+6r^2+2\right)b'(r)+r\left(r^2+1\right)^2 b''(r)\Big] \qquad (5.6.6)\end{aligned}$$

$$\begin{aligned}\bar{p}_r &= -\frac{1}{R^3 r\left(r^2+1\right)\left(c_1-c_2+r^2\left(c_1+c_2\right)\right)^2}\\ &\quad\Big[16c_2 e^{\lambda t}R^3 r\left(r^2-1\right)a(r)\\ &\quad+\left(r^2+1\right)\{2r\left(r^2+1\right)\\ &\quad\langle c_1^2\left(r^2+1\right)^2\left(r^2+2e^{\lambda t}-1\right)\\ &\quad+c_2^2\left(r^2-1\right)\left(r^4-6r^2+1+6e^{\lambda t}\left(r^2-1\right)\right)\\ &\quad+2c_1c_2\left(r^6+1+4e^{\lambda t}\left(r^4-1\right)-3r^2\left(r^2+1\right)\right)\\ &\quad-2e^{\lambda t}R^2\lambda^2\left(r^2+1\right)^2\rangle b(r)\\ &\quad+\left(c_1-2c_2+r^2\left(c_1+c_2\right)\right)\\ &\quad\Big(-4e^{\lambda t}R^3\left(r^2-1\right)a'(r)+\left(r^2+1\right)^2\\ &\quad\left(-c_1+c_2-6c_2r^2+r^4\left(c_1+c_2\right)\right)b'(r)\Big)\}\Big] \qquad (5.6.7)\end{aligned}$$

$$
\begin{aligned}
\bar{p}_t &= -\frac{e^{\lambda t}\left(r^2+1\right)}{8R^3 r\left(c_1-c_2+r^2\left(c_1+c_2\right)\right)^2} \\
&\quad \left[16c_2 Rr\left(r^2-1\right)a(r)\right. \\
&\quad +\{4r\langle c_1^2\left(r^2+1\right)^2\left(r^2+3\right) \\
&\quad +c_2^2\left(r^4-2r^2+1\right)\left(r^2+7\right) \\
&\quad +2c_1c_2\left(r^6+5r^4-r^2-5\right) \\
&\quad -2R^2\lambda^2\left(r^2+1\right)^2\rangle b(r) \\
&\quad +\left(r^2+1\right)\left(c_1-c_2+r^2\left(c_1+c_2\right)\right) \\
&\quad \langle 2R\left(r^2+1\right)a'(r) \\
&\quad +\left(5r^2+1\right)\left(c_1-c_2+r^2\left(c_1+c_2\right)\right)b'(r) \\
&\quad +2Rr\left(r^2+1\right)a''(r) \\
&\quad \left.+\left(\left(r^3+r\right)\left(c_1-c_2+r^2\left(c_1+c_2\right)\right)\right)b''(r)\rangle\}\right]
\end{aligned}
\tag{5.6.8}
$$

$$
\begin{aligned}
Q &= -\frac{\lambda e^{\lambda t}\left(r^2+1\right)^2}{2R^2\left(c_1-c_2+r^2\left(c_1+c_2\right)\right)^2} \\
&\quad \times\left[2r\left(c_1-3c_2+r^2\left(c_1+c_2\right)\right)b(r)\right. \\
&\quad \left.+\left(r^2+1\right)\left(c_1-c_2+r^2\left(c_1+c_2\right)\right)b'(r)\right]
\end{aligned}
\tag{5.6.9}
$$

where we have written $Q = qB$. We note that (5.6.6) - (5.6.9) contain two unspecified quantities, namely $a(r)$ and $b(r)$. Following Chan *et al* (1993) we adopt the following form for $b(r)$

$$
b(r) = (1+\xi f(r))\, A_0 B_0 \tag{5.6.10}
$$

where we choose $f(r) = r^2$. Then equation (5.5.13) together with (5.6.10) can be expressed as

$$
qB = \frac{2}{B_0}\xi f' \dot{T} \tag{5.6.11}
$$

Note that, for our choice of $f(r)$, $f'(r) = 2r$ which is positive. Also note that $\dot{T} < 0$ because the fluid is collapsing. Since heat flux is positive, it follows that $\xi < 0$.For dissipative collapse $\xi \neq 0$, for $\xi = 0$ would imply zero heat flow.

In order to determine $a(r)$ we impose an equation of state of the form

$$\bar{p}_r = \gamma \bar{\mu} \tag{5.6.12}$$

which yields

$$\begin{aligned}
0 \quad = \quad & \frac{1}{Rr\left(r^2+1\right)\left(c_1-c_2+r^2\left(c_1+c_2\right)\right)} \\
& \Big[-4c_2 r\left(r^2-1\right)\left(\left(r^2+1\right)^3\right)a(r) \\
& +\left(c_1-c_2+r^2\left(c_1+c_2\right)\right) \\
& \{2r\langle\left(2R^2\lambda^2\left(\left(1+r^2\right)^3\right)\left(1+r^2\xi\right)\right) \\
& +2c_1c_2\left(1+r^2\right)\left[\left(3+9\gamma+6R\gamma\left(-2+\xi\right)+\xi\right)\right. \\
& +r^8\xi-r^6\left(5+\left(9+2R\right)\gamma\right)\xi-r^4\left(3+6\xi+\left(9+2R\xi\right)\gamma\right) \\
& \left.+r^2\left(6R\gamma\left(2-3\xi\right)+\xi+9\gamma\xi\right)\right] \\
& +c_1^2\left(\left(r^2+1\right)^2\right)\left[-2-\xi+r^6\xi-r^4\left(1+\left(9+2R\right)\gamma\right)\xi\right. \\
& \left.-r^2\left(2+3\xi+\left(9+9\xi+2R\xi\right)\gamma\right)+\left(-9+6R-6R\xi\right)\gamma\right] \\
& +c_2^2\left[-4-\xi+r^10\xi-r^8\left(9+9\gamma+2R\gamma\right)\xi\right. \\
& -r^6\left(4+10\xi+\left(9-9\xi+2R\xi\right)\gamma\right) \\
& +r^4\left(-4+2\xi+\left(9+18R+9\xi-28R\xi\right)\gamma\right) \\
& \left.+r^2\left(-4+\xi+\left(9-36R-9\xi+38R\xi\right)\gamma\right)\right]\rangle \\
& +\left(r^2-1\right)\left(\left(r^2+1\right)^4\right)a'(r)\}\Big]
\end{aligned} \tag{5.6.13}$$

The above equation (5.6.13) is a first order linear differential equation in $a(r)$ which has the solution

$$
\begin{aligned}
a(r) \;=\;& \frac{1}{2\left(r^2+1\right)}\left(c_1-c_2+r^2\left(c_1+c_2\right)\right) \\
& \left[-\frac{18c^2R\gamma\left(\xi-1\right)}{\left(r^2+1\right)^2}\right. \\
& -\left(2\left(c_1+c_2\right)\left(r^2-1\right)\xi\right) \\
& +\frac{1}{r^2+1}\{6c_1R\gamma\left(\xi-1\right) \\
& +2c_2\left(-2-9\gamma+\left(2+\left(9+6R\right)\gamma\right)\xi\right)\}+2c_1 \\
& +\frac{1}{c_1}\{4c_1c_2\left(1+2R\gamma\right)\xi+2\left(c_2-R\lambda\right)\left(c_2+R\lambda\right)\left(1-\xi\right) \\
& +c_1^2\left(2\left(1+\xi\right)+\left(9-3R+9\xi+5R\xi\right)\gamma\right)\}\log\left(r^2-1\right) \\
& -\{c_1\left(4+\gamma\left(9-3R+R\xi-9\xi\right)-4\xi\right) \\
& +2c_2\left(-6+\left(-9+2R\right)\gamma\right)\xi\}\log\left(r^2+1\right) \\
& -\frac{1}{c_1\left(c_1+c_2\right)}\{2\left(c_1^2-c_2^2+R^2\lambda^2\right)\left(c_1\left(\xi-1\right)-c_2\left(\xi+1\right)\right) \\
& \left.\log\left(c_1-c_2+r^2\left(c_1+2\right)\right)\}\right]
\end{aligned}
\tag{5.6.14}
$$

This completes the model.

We can now rewrite the following

$$
\begin{aligned}
\bar{\mu} \;=\;& \frac{e^{\lambda t}}{R^2}\left[6c_1+\{3c_1-3c_2+10r^2\left(c_1+c_2\right)\right. \\
& \left.+r^4\left(c_1+c_2\right)\}\xi\right]7a\text{"}ls)
\end{aligned}
\tag{5.6.15}
$$

$$
\begin{aligned}
\bar{p}_r \quad = \quad & \frac{1}{R^2\left(r^2+1\right)^4\left(c_1-c_2+r^2\left(c_1+c_2\right)\right)} \\
& \Big[\{2e^{\lambda t}\left(\left(r^2+1\right)^3\right)\left(r^2\xi+1\right)R^2 \\
& \left(-2R^2k_1-4R^2k_2^2+4R^2k_2\sqrt{k_1+k_2^2}+\lambda^2\left(r^2+1\right)^2\right)\} \\
& -2c_1c_2\left(r^2+1\right)\{\left(r^2+1\right)^3 \\
& \left(-1+\xi+r^2+\left(r^4-2r^2-4\right)r^2\xi\right) \\
& +2e^{\lambda t}\langle -2+3R^2+3R^2\left(3-4R+2R\xi\right)\gamma+R^2\xi \\
& +2r^{10}\xi+r^8\left(2+4\xi+R^2\xi\right) \\
& +r^6\left(4-5R^2\xi-R^2\xi\left(9+2R\right)\gamma\right) \\
& -r^4\left(4\xi+3R^2+6R^2\xi+R^2\left(9+2R\xi\right)\gamma\right) \\
& +r^2\left(-4-2\xi+6R^3\left(2-3\xi\right)\gamma+R^2\xi+9R^2\gamma\xi\right)\rangle\} \\
& -c_1^2\left(r^2+1\right)^2\{\left(r^2-1\right)\left(r^2+1\right)^4\xi \\
& +2e^{\lambda t}\langle -1-2R^2-R^2\xi-R^2\left(9-6R+6R\xi\right)\gamma \\
& +r^8\xi+r^6\left(1+3\xi+R^2\xi\right) \\
& +r^4\left(3+3\xi-R^2\xi-r^2\xi\left(9+2R\right)\gamma\right) \\
& +r^2\left(3+\xi-2R^2-3R^2\xi-r^2\left(9+9\xi+2r\xi\right)\gamma\right)\rangle\} \\
& +c_2^2\{-\left(r^2+1\right)^3\left(r^4-6r^2+1\right)\left(2+\left(r^4+2r^2-1\right)\xi\right) \\
& -2e^{\lambda t}\langle 3-4R^2-3R^2\left(3-6R+2R\xi\right)\gamma-R^2\xi \\
& +3r^{12}\xi+r^{10}\left(3+3\xi+R^2\xi\right) \\
& -r^8\left(-3+6\xi+R^2\xi\left(9+9\gamma+2R\gamma\right)\right) \\
& -r^6\left(6+6\xi+4R^2+9R^2\gamma+R^2\xi\left(10-9\gamma+2R\gamma\right)\right) \\
& +r^4\left(3\xi-6+2R^2\xi-4R^2+R^2\left(9+18R+9\xi-28R\xi\right)\gamma\right) \\
& +r^2\left(3+3\xi-4R^2+R^2\xi\right. \\
& \left.+R^2\left(9-36R-9\xi+38R\xi\right)\gamma\right)\rangle\}\Big] \qquad (5.6.16)
\end{aligned}
$$

$$
\begin{aligned}
\bar{p}_t \;=\; & -\frac{e^{\lambda t}}{R^2\left(r^4-1\right)\left(c_1-c_2+r^2\left(c_1+c_2\right)\right)^2} \\
& \Big[c_1^2 c_2\left(r^2+1\right)^2\{3\gamma\left(r^2-1\right)^2\left(9-9r^4-10R+20r^2R\right) \\
& +2r^2\xi\left(3r^8-10r^4-8r^2-1\right) \\
& +2\gamma\xi\left(27r^2\left(r^2-1\right)^2\left(r^2+1\right)\right) \\
& +2R\gamma\xi\left(4r^8-48r^6+61r^4-58r^2+9\right)\} \\
& -c_2\left(r^2-1\right)^2\{2R^2\lambda^2\left(r^2-1\right)\left(r^2+1\right)^3 \\
& +9c_2^2\gamma\left(r^2-1\right)\left(1-2R-5r^2-5r^4+r^6-4Rr^4+14Rr^2\right) \\
& -2c_2^2\xi\langle\left(r^3+r\right)^2\left(r^4+10r^2-3\right) \\
& +3R\gamma+r^8\gamma\left(4R+27\right)-3r^6\gamma\left(8R+3\right) \\
& +9r^4\gamma\left(11R-3\right)+r^2\gamma\left(-50R+9\right)\rangle \\
& +2r^2R^2\lambda^2\left(r^2-1\right)\left(r^2+1\right)^3+R^2\left(r^2+1\right)^3\left(1-r^2+2r^2\xi\right) \\
& \langle 2k_1+4k_2^2-4k_2\sqrt{k_1+k_2^2}\rangle\} \\
& +c_1^3\left(r^2+1\right)^3\{-3\gamma\left(3-2R+2R\xi\right)+2r^8\xi \\
& -r^6\left(9\gamma+6\xi\right)-r^4\left(4+6\xi+\gamma\left(9+18\xi-12R+16R\xi\right)\right) \\
& +r^2\left(-4-9\gamma-6R\gamma-2\xi+2\gamma\xi\left(R-9\right)\right)\} \\
& +c_1\left(r^2+1\right)\{-2R^2\left(r^2+1\right)^3 \\
& \langle\lambda^2\left(r^2-1\right)^2\left(r^2\xi+1\right) \\
& +\left(r^4+2r^2\xi+1\right)\left(-k_1-k_2^2+2k_2\sqrt{k_1+k_2^2}\right)\rangle \\
& +c_2^2\langle-3\gamma\left(9-14R+6R\xi\right)+6r^{12}\xi \\
& +r^{10}\left(22\xi-27\gamma+4\gamma\xi\left(4R+27\right)\right) \\
& +r^8\left(4-24\xi+135\gamma+84R\gamma-18\gamma\xi\left(8R+9\right)\right) \\
& 2r^6\left(-10+24\xi-54\gamma-27\gamma\xi+R\gamma\left(-189+215\xi\right)\right) \\
& +2r^4\left(-10+\xi+3\gamma\left(-18+91R+27\xi-85R\xi\right)\right) \\
& +r^2\left(4+10\xi+\gamma\left(135-294R-54\xi+226R\xi\right)\right)\rangle\}\Big]
\end{aligned}
\tag{5.6.17}
$$

$$Q = -\frac{2e^{\lambda t} r \left(r^2+1\right) \lambda \xi}{R} \tag{5.6.18}$$

5.7 Stability

The stability of a star undergoing dissipative collapse has been studied by several authors over the past three decades. The role of pressure anisotropy and the presence of radiation within the stellar core affects the stability factor, Γ. It was shown that a change in sign in the anisotropy parameter can render the core unstable as can be deduced from the Newtonian limit

$$\Gamma < \frac{4}{3} + \left[-\frac{4}{3}\frac{(p_{r0} - p_{t0})}{|p'_{r0}| r} + \frac{2}{3}\alpha_{\Sigma}\xi \frac{|f'|}{|p'_{r0}|} \right]_{max} \tag{5.7.1}$$

However, we have elected to base this work on an isotropic static model in order to determine the link between the stability index Γ and the equation of state parameter γ. Relativistic contributions from the energy density predicts a stability factor different from its Newtonian counterpart, given by

$$\Gamma < \frac{4}{3} + \left[-\frac{4}{3}\frac{(p_{r0} - p_{t0})}{|p'_{r0}| r} + \frac{1}{3}\frac{\mu_0 p_{r0}}{|p'_{r0}|} r + \frac{2}{3}\alpha_{\Sigma}\xi \frac{|f'|}{|p'_{r0}|} - \frac{1}{3}\mu_0 \frac{\xi |f'|}{|p'_{r0}|} \right]_{max} \tag{5.7.2}$$

Figure 5.1 shows the stability factor in the Newtonian regime, when the star is close to hydrostatic equilibrium. During this stage the energy emission from the core is small and we expect the star to be stable from the centre outwards towards its surface. Figure 5.1 shows us that the different matter configurations all possess $\Gamma > \frac{4}{3}$ indicating that the core is stable. It is interesting to note that there is a deviation for different EoS parameter (γ) as one approaches the surface of the star. The so-called 'dark'stars corresponding to the blue and brown curves are more stable than the stars composed of baryonic matter. We also observe that the surface layers are more stable than the inner core region of the star. We expect this as the outer layers are cooler than the central regions. Figure 5.2 displays the stability factor for the Post-Newtonian limit. This epoch corresponds to the late stage collapse of the star. During this period we expect the core to be dynamically unstable. It is clear from Figure 5.2 that different configurations (varying γ) are unstable at the centre with the baryonic matter configurations having $\Gamma_{centre} < 4/3$ and dark star models having $\Gamma_{centre} = 4/3$. As we move away from the central regions of the star the stability index increases to above the critical value of 4/3. Again, we observe that the collapse with the loss of energy in the form of a radial heat flux drives the dark energy stars to increased stability as compared to their baryonic counterparts. Our analysis of the stability factor clearly indicates the strong connection between the equation of state parameter (γ) and the stability of the stellar configuration.

It has been shown in Herrera *et al* (2010) that the scalar function

$$\mathcal{Y}_{TF} = 16\pi\eta\sigma + \frac{4\pi}{R^3}\int_0^R R^3\left(D_R\mu - 3q\frac{U}{RE}\right)dR \tag{5.7.3}$$

where σ is the shear scalar, $D_R = \frac{1}{R'}\frac{\partial}{\partial r}$ is the proper radial derivative, $D_T = \frac{1}{A}\frac{\partial}{\partial t}$ is the proper time derivative, $U = D_T R < 0$ and

$$E = \left(1 + U^2 - \frac{2m}{R}\right)^{1/2}$$

is the mass function measures the stability of the shear-free condition. We note that $\mathcal{Y}_{TF}$ is a combination of shear viscosity, pressure anisotropy, inhomogeneities in the density and the heat flux. The presence of the dissipative flux, anisotropy and inhomogeneity can lead to deviation from the shear-free profile as the collapse proceeds. From observation of the various terms in (5.7.3) it is quite clear that even in the absence of shear viscosity (the vanishing of the internal friction between the adjacent fluid layers of the collapsing fluid) there can be an increase in the absolute value of the shear scalar due to the presence of density inhomogeneity and heat flux. Since shear-free profiles are unstable in the presence of dissipation, anisotropy and inhomogeneity, the invoking of the shear-free condition may be valid for a limited timescale during the collapse process.

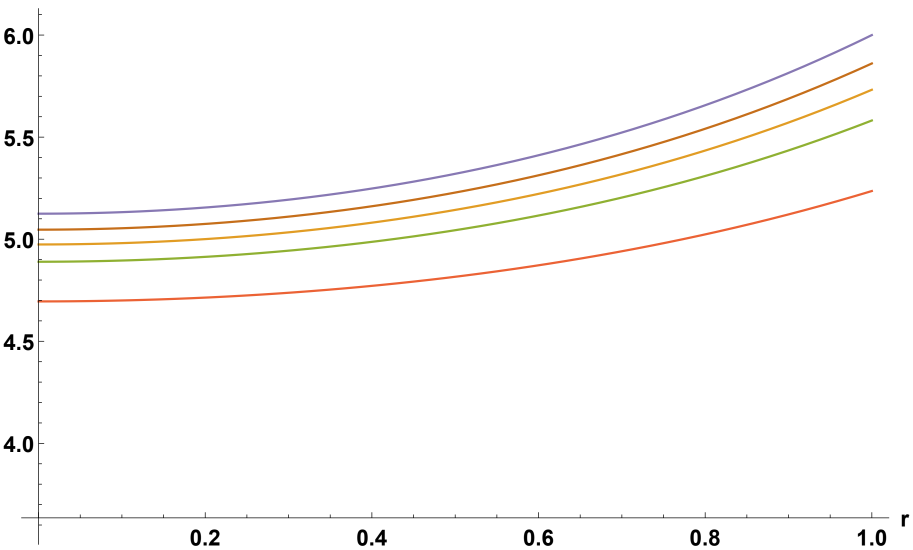

Figure 5.1: Stability factor Γ as a function of the radial coordinate r for the Newtonian limit. Blue: $\gamma = -1$, Brown: $\gamma = -\frac{1}{3}$, Orange: $\gamma = 0$, Green: $\gamma = \frac{1}{3}$, Red: $\gamma = 1$

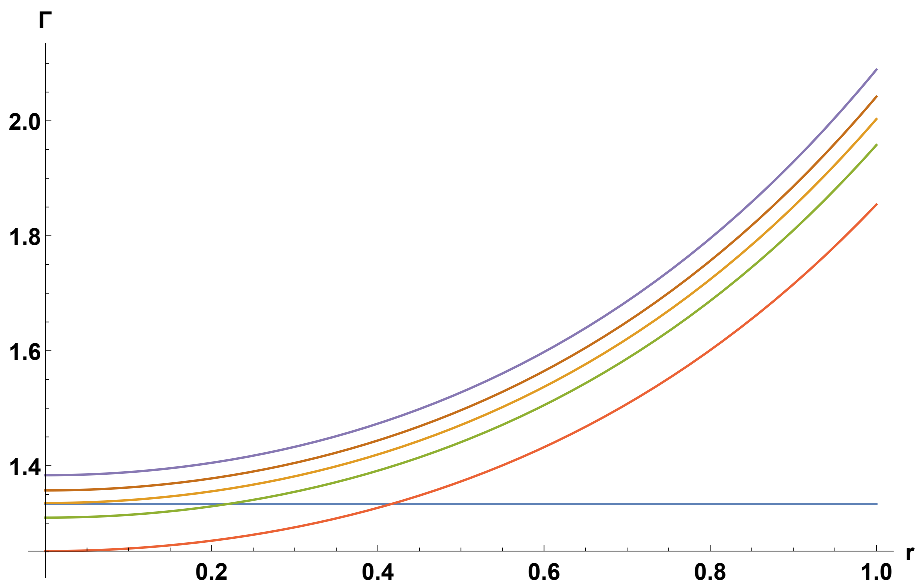

Figure 5.2: Stability factor Γ as a function of the radial coordinate r for the Post-Newtonian limit. Blue: $\gamma = -1$, Brown: $\gamma = -\frac{1}{3}$, Orange: $\gamma = 0$, Green: $\gamma = \frac{1}{3}$, Red: $\gamma = 1$

5.8 Discussion

In this work we investigated the effect of an equation of state on the dynamical stability or instability of a spherically symmetric star undergoing dissipative collapse. A perturbative approach was adopted in which the star starts collapsing from an initial static configuration in the infinite past ($t = -\infty$). The radial perturbation in the gravitational potential was determined by specifying a linear equation of state of the form $p_r = \gamma\mu$. The temporal evolution of the model was determined from the junction conditions. It was shown that the temporal behaviour of the model is intrinsically linked to the equation of state parameter, γ. The stability of our model was studied by investigating the stability index and its dependence on γ. We were in a position to clearly show the variation of the stability index with the equation of state parameter throughout the stellar fluid. More importantly, our investigation revealed that the stability depends on the nature of the matter making up the stellar interior. Our results are new and contribute to recent findings by Naidu *et al* (2016) and Govender *et al* (2016) in which they found that the equation of state affects the end state of collapse and temperature profiles of the radiating body.

Chapter 6

Conclusion

We now provide an overview of the main results obtained during the course of our investigations:

- In Chapter 2 the general mathematical preliminaries required for the dissertation were outlined.

- In Chapter 3 the method of conformal mappings was employed to obtain simple static and nonstatic solutions which displayed pleasing properties in respect of the energy density, pressure, energy conditions and stability of the conformally related metric. These solutions have the potential to generate physically realistic astrophysical models.

- In Chapter 4 we utilised the plane symmetric anisotropic Kasner metric as a seed solution and, through a conformal mapping, generated two classes of solutions that modeled universes filled with perfect fluid with isotropic particle pressure. Both sets of solutions represented models that were accelerating, shearing and nonrotating. However one of the models was expanding while the other was in collapse. The exact solutions obtained may prove to be useful in the study of gravitational waves. Future research on this topic could focus on obtaining new classes of anisotropic solutions by relaxing the isotropy condition.

- The focus of Chapter 5 was a spherically symmetric, shear-free static configuration undergoing radiative collapse. Employing a perturbative scheme, we investigated the influence of a linear equation of state on the dynamical (in)stability of the sphere in the Newtonian and post-Newtonian regimes. Our plots revealed that the stability of our model is dependent on the equation of state parameter γ. Different values of γ representing the various matter configurations produced varying degrees of stability at the core and at the surface of the star. This is a new result. Future work on this topic could include the presence of shear.

Bibliography

[1] Abbot B P *et al*, Observation of gravitational waves from a binary black hole merger, *Phys. Rev. Lett* **116**, 061102 (2016).

[2] Anderson R L and Ibragimov N H, Lie-Backlund Transformations in Applications, (Philadelphia: SIAM) (1979).

[3] Anguige K, A class of plane symmetric perfect fluid cosmologies with a Kasner-like singularity, *Class. Quant. Grav.* **17**, 2117 (2000).

[4] Ashtekar A, Tomasz P and Singh P, Quantum nature of the big bang, *Phys. Rev. Lett.* **96**, 141301 (2006).

[5] Bari P, Bhattacharya K and Chakraborty S, Causal horizons in a bouncing universe, *Gen. Rel. Grav.* **50**, 118 (2018).

[6] Belinskii V A, Khalatnikov I M and Lifshitz E M, A general solution of the Einstein equations with a time singularity *Adv. Phys.* **31**, 639 (1982).

[7] Birkhoff G D, Relativity and Modern Physics., (Cambridge, MA: Harvard University Press) (1923).

[8] Bluman G W and Kumei S, Symmetries and Differential Equations, (New York: Springer- Verlag) (1989).

[9] Bojowald M, What happened before the big bang?, *Nat. Phys.* **3**, 523 (2007).

[10] Bonnor W B, de Oliveira A K G and Santos N O, Radiating spherical collapse, *Phys. Rep.* **181**, 269 (1989).

[11] Boonserm P, Visser M and Weinfurtner S, Generating perfect fluid spheres in general relativity, *Phys. Rev. D.* **71**, 124037 (2005).

[12] Buchdahl H A, Conformal flatness of the Schwarzschild interior solution, *American J. Phys.* **39(2)**, 158 (1971).

[13] Cahill M E and Taub A H, Spherically symmetric similarity solutions of the Einstein field equations for a perfect fluid, *Commun. Math. Phys.* **21**, 1 (1971).

[14] Cai Y, Damien E and Brandenberger R, Towards a nonsingular bouncing cosmology, *J. Cosmol. Astropart. Phys.* **8**, 020 (2012).

[15] Castejon-Amenedo J and Coley A A, Exact solutions with conformal Killing vector fields, *Class. Quant. Grav.* **9**, 2203 (1992).

[16] Chan R, Radiating gravitational collapse with shear viscosity, *Mon. Not. R. Astron. Soc.* **316**, 588 (2000).

[17] Chan R, Herrera L and Santos N O, Dynamical instability for radiating anisotropic collapse, *Mon. Not. R. Astron. Soc.* **265**, 533 (1993).

[18] Chandrasekhar S, The dynamical instability of gaseous masses approaching the Schwarzschild limit in general relativity, *Astrophys. J.* **140**, 417 (1964).

[19] Coley A A and Czapor S R, Plane symmetric spacetimes admitting inheriting conformal Killing vector fields, *Class. Quant. Grav.* **9**, 1787 (1992).

[20] Coley A A and Tupper B O J, Spherically symmetric anisotropic fluid ICKV spacetimes, *Class. Quant. Grav.* **11**, 2553 (1994)

[21] Collins C B, Static relativistic perfect fluids with spherical, plane or hyperbolic symmetry, *J. Math. Phys.* **26**, 2268 (1985).

[22] Dadhich N K, Inhomogenous imperfect fluid spherical models without big bang singularity, *J.Astrophys.Astron.* **18**, 343 (1997).

[23] Dadhich N K and Raychaudhuri A K, Oscillating nonsingular relativistic spherical model, *Mod.Phys.Lett. A.* **14**, 2135 (1999).

[24] Davis T M and Ray J R, Ghost neutrinos in plane symmetric spacetimes, *J. Math. Phys.* **16**, 75 (1975).

[25] de Felice F and Clarke C J S, Relativity on Manifolds (Cambridge: Cambridge University Press) (1990).

[26] Defrise-Carter L, Conformal groups and conformally equivalent isometry groups, *Commun. Math. Phys.* **40**, 273 (1975).

[27] Delgaty M S R and Lake K, Physical acceptability of isolated, static, spherically symmetric, perfect fluid solutions of Einstein's equations, *Comp. Phys. Comm.* **115**, 395 (1998).

[28] de Oliveira A K G and Santos N O, Nonadiabatic gravitational collapse, *Astrophys. J.* **312**, 640 (1987).

[29] de Oliveira A K G, Santos N O and Kolassis C A, Collapse of a radiating star, *Mon. Not. R. Astron. Soc.* **216**, 1001 (1985).

[30] Engelhardt N, Hertog T and Horowitz G T, Further holographic investigations of big bang singularities, *J. High Energy Phys.* **2015**, 29044 (2015).

[31] Fodor G, Generating spherically symmetric static perfect fluid solutions, arXiv:gr-qc/0011040v1 (2000).

[32] Fukushima M, Gravitational baryogenesis after anisotropic inflation, *Phys. Rev. D.* **93**, 103513 (2016).

[33] Govender M, Bogadi R and Maharaj S D, The influence of an equation of state during radiative collapse, *Int. J. Mod. Phys. D.* **26**, 1750065 (2016).

[34] Govender M, Govinder K S, Maharaj, S D, Sharma R, Mukherjee S and Dey T K, Radiating spherical collapse with heat flow, *Int. J. Mod. Phys. D.* **12**, 667 (2003).

[35] Govender M, Mewalal N and Hansraj S, The role of an equation of state in the dynamical (in)stability of a radiating star, *Eur. Phys. J. C.* **79**, 24 (2019).

[36] Govender M, Reddy K P and Maharaj S D, The role of shear in dissipative gravitational collapse, *Int. J. Mod. Phys. D.* **23**, 1450013 (2014).

[37] Govender M and Thirukkanesh S, Causal heat flow in Bianchi type-V universe, *Phys. Lett. A.* **29**, 1450071 (2014).

[38] Govinder, K S and Hansraj S, Group analysis of a conformal perfect fluid spacetime, *J. Phys. A.* **45**, 155210 (2012).

[39] Grøn Ø and Soleng H H, Static plane symmetric spacetime with a conformally coupled massless scalar field, *Phys. Lett. A.* **165**, 191 (1992).

[40] Hall G S and Steele J D, Conformal vector fields in general relativity, *J. Math. Phys.* **32**, 1847 (1991).

[41] Hansraj S, Perfect fluid metrics conformal to the Schwarzschild exterior spacetime, *Gen. Rel. Grav.* **44**, 125 (2012)

[42] Hansraj S, Plane symmetric relativistic fluids with Taub geometry, *Eur. Phys. J. Plus* **128**, 120 (2013)

[43] Hansraj S, Govender M and Mewalal N, Expanding, shearing and accelerating isotropic plane symmetric universe with Kasner geometry, *Mod. Phys. Lett. A.* **33**, 1850143 (2018).

[44] Hansraj S, Govinder K S and Mewalal N, Conformal mappings in relativistic astrophysics, *J. Appl. Math* **2013**, 196385 (2013).

[45] Hansraj S, Maharaj S D, Msomi A M and Govinder K S, Lie symmetries for equations in conformal geometries, *J. Phys. A: Math. and Gen.* **38**, 4419 (2005).

[46] Hawking S W and Ellis G F R, The large scale structure of spacetime, (Cambridge: Cambridge University Press) (1973).

[47] Hawking S W and Penrose R, The singularities of gravitational collapse and cosmology, *Proceedings of the Royal Society A* **314**, 529 (1970).

[48] Head AK, Program LIE for Lie analysis of differential equations on IBM type PCs, *Comp Phys Comm* **77**, 241 (1993).

[49] Herrera L, di Prisco A, Fuenmayor E and Troconis O, Dynamics of viscous dissipative collapse: A full causal approach, *Int. J. Mod. Phys. D.* **18**, 129 (2009).

[50] Herrera l, di Prisco A and Ospino J, On the stability of the shear-free condition, *Gen. Rel. Grav.* **42**, 1585 (2010).

[51] Herrera L, Le Denmat G and Santos N O, Dynamical instability for nonadiabatic spherical collapse, *Mon. Not. R. Astron. Soc.* **237**, 257 (1989).

[52] Herrera L, Le Denmat G. and Santos N O, Dynamical instability and the expansion-free condition, *Gen. Rel. Grav.* **44**, 1143 (2012).

[53] Herrera L, Santos N O and Wang A, Shearing expansion-free spherical anisotropic fluid evolution, *Phys. Rev. D.* **78**, 084026 (2008).

[54] Ibragimov N H, CRC Handbook of Lie group analysis of differential equations Vol 2, (Boca Raton: CRC Press) (1995).

[55] Jebsen J T, *Über die allgememeinen kugelsymmetrischen Losungen der Einsteinschen Gravitationsgleichungen im Vakuum* , *Ark. Mat. Astron. Fys.* **15**, 18 (1921).

[56] Joshi P S, *Global Aspects in Gravitation and Cosmology*, (Oxford: Clarendon Press) (1993).

[57] Kasner E, *Geometrical theorems of Einstein's cosmological equations*, *American J. Math.* **43**, 217 (1921).

[58] Katzin G H and Levine J, *Applications of Lie derivatives to symmetries, geodesic mappings and first integrals in Riemannian spaces*, *Coll. Math.* **XXVI** 21 (1972).

[59] Katzin G H, Levine J and Davis W R, *Curvature collineations: A fundamental symmetry property of the spacetimes of general relativity defined by the vanishing Lie derivative of the Riemann curvature tensor*, *J. Math. Phys.* **10**, 617 (1969).

[60] Kerr R P, *Gravitational field of a spinning mass as an example of algebraically special metrics*, *Phys. Rev. Lett.* **5**, 237 (1963).

[61] Knutsen H, *Nonstatic gas spheres in general relativity*, *Gen. Rel. Grav.* **16**, 777 (1984).

[62] Kolassis C A, Santos N O and Tsoubelis D, *Friedmann-like collapsing model of a radiating sphere with heat flow*, *Astrophys. J.* **327**, 755 (1988).

[63] Kramer D, Spherically symmetric radiating solution with heat flow in general relativity, *J. Math. Phys.* **33**, 1458 (1992).

[64] Lake K, V^{th} Brazilian School of Cosmology and Gravitation, Edited by M Novello, (Singapore: World Scientific) (1987).

[65] Lake K, All static spherically symmetric perfect fluid solutions of Einstein's equations, *Phys. Rev. D.* **67**, 104015 (2003).

[66] LeFloch P G and Tchapnda S B, Plane symmetric spacetimes with positive cosmological constant: The case of stiff fluids, *Adv. Theor. Math. Phys.* **15**, 1 (2011).

[67] Maharaj S D and Govender M, Collapse of a charged radiating star with shear, *Pramana-J. Phys.* **54**, 715 (2000).

[68] Martin D and Visser M, Algorithmic construction of static perfect fluid spheres, *Phys. Rev. D.* **69**, 104028 (2004).

[69] Maurya S K, Banerjee A and Hansraj S, Role of pressure anisotropy on relativistic compact stars, *Phys. Rev. D.* **97**, 044022 (2018).

[70] Misner C W, Mixmaster universe, *Phys. Rev. Lett.* **22**, 1071 (1969).

[71] Misner C W and Sharp D, Relativistic equations for adiabatic, spherically symmetric gravitational collapse, *Phys. Rev. B.* **136**, 571 (1964).

[72] Misner C W, Thorne K S and Wheeler J A, Gravitation, (San Francisco: W H Freeman) (1973).

[73] Moroi T and Murayama H, CMB anisotropy from baryogenesis by scalar field, *Phys. Lett. B.* **553**, 126 (2003).

[74] Naidu N F and Govender M, The influence of initial conditions during dissipative collapse, *Int. J. Mod. Phys. D.* **25**, 1650092-434 (2016)

[75] Nariai H, A simple model for gravitational collapse with pressure gradient, *Prog. Theor. Phys.* **38**, 92 (1967).

[76] Newman E, Couch E, Chinnapared K, Exton A, Prakash A and Torrence R, Metric of a rotating, charged mass, *J. Math. Phys* **6** 918 (1965)

[77] Nørdstrom G, On the energy of the gravitational field in Einstein's theory, *Proc. K. Ned. Akad. Wet.* **20**, 1238 (1918).

[78] Oppenheimer J R and Snyder H, On continued gravitational contraction, *Phys. Rev.* **56**, 455 (1939).

[79] Oppenheimer J R and Volkoff G, On massive neutron cores, *Phys. Rev.*, **55**, 374 (1939).

[80] Patel L K and Dadhich N K, Singularity-free inhomogenous models with heat flow, *Class. Quant. Grav.* **10**, L85 (1993).

[81] Peebles P J E and Ratra B, The cosmological constant and dark energy, *Rev. Mod. Phys.* **75**, 559 (2003).

[82] Penrose R, Gravitational collapse and spacetime singularities, *Phys. Rev. Lett.* **14**, 57 (1965).

[83] Petrov A Z, Classification of spaces defined by gravitational fields (English translation), *Gen. Rel. Grav.* **32** 1665 (1954)

[84] Pfister H, On the history of the so-called Lense-Thirring effect, *Gen. Rel. Grav.* **39**, 1735 (2007)

[85] Rahman S and Visser M, Spacetime geometry of static fluid spheres, *Class. Quant. Grav.* **19**, 935 (2002).

[86] Reissner H, *Ü*ber die Eigengravitation des elektrischen feldes nach der Einsteinschen theorie, *Ann. Phys. Lpz.* **50**, 106 (1916).

[87] Roy S R and Narain S, Some plane symmetric models of perfect fluid distribution in general relativity, *Indian J. pure appl. Math.* **10**, 763 (1979).

[88] Saaidi Kh and Hossienkhani H, Gravitational baryogenesis in anisotropic universe, *Astroph. Space Sci.* **333**, 305 (2011).

[89] Santos N O, Nonadiabatic radiating collapse, *Mon. Not. R. Astron. Soc.* **216**, 403 (1985).

[90] Schutz B F, A first course in general relativity, (Cambridge: Cambridge University Press) (2009).

[91] Schwarzschild K, Über das Gravitationsfeld eines Massenpunktes nach der Einsteinchen Theorie, *Sitzungsber Preuss. Akad. Wiss. Phys. Math.* **K1**, 189 (1916a).

[92] Schwarzschild K, Über das Gravitationsfeld einer Kügel aus inkompressibler Flussgkeit nach der Einsteinschen Theorie, *Sitzungsber Preuss. Akad. Wiss. Phys. Math.* **K1**, 424 (1916b).

[93] Sharif M, Classification of static plane symmetric spacetimes according to their matter collineations, *J. Math. Phys.* **45**, 1518 (2004).

[94] Sharif M and Siddiqa A, Singularity in gravitational collapse of plane symmetric charged Vaidya spacetime, *Mod. Phys. Lett. A* **25**, 2831 (2010).

[95] Stephani H, Konform flache gravitationsfelde, *Commun. Math. Phys.* **5**, 337 (1967).

[96] Stephani H, Kramer D, MacCallum C A H, Hoenselaers C and Herlt E, Exact solutions of Einstein's field equations, (Cambridge: Cambridge University Press) (2003)

[97] Taub A H, Empty spacetimes admitting a three parameter group of motions, *Annals Math.* **53**, 472 (1951).

[98] Tikekar R, A note on plane symmetric perfect fluid distributions of embedding class one, *Indian J. pure appl. Math* **11**, 1681 (1980).

[99] Tolman R C, Static solutions of Einstein's field equations for spheres of fluid, *Phys. Rev.* **55**, 364 (1939).

[100] Tomimura M A and Nunes F C P, Radiating spherical collapse with shear and heat flow, *Astrophys. Space Sci.* **199**, 215 (1993).

[101] Vaidya P C, The gravitational field of a radiating star, *Proc. Indian Acad. Sc. A* **33**, 264 (1951).

[102] Wyman M, Radially symmetric distributions of matter, Phys. Rev. **75**, 1930 (1949).

[103] Zhang H S and Noh H, n-dimensional plane symmetric solution with perfect fluid source, *Phys. lett. B* **671**, 428 (2009).